

5 HIGHLIGHTS OF LABORATORY FOR ATMOSPHERES ACTIVITIES

This section highlights some of the Laboratory's research accomplishments for 2002. The section is partitioned by Branch. A Branch summary, written by the respective Branch Head is followed by one or more science highlight articles. The Branch Web sites can be accessed from the Laboratory for Atmospheres Web site at <http://atmospheres.gsfc.nasa.gov/>.

Data Assimilation Office (DAO), Code 910.3

Branch Summary

The DAO's accomplishments in 2002 include:

1. An upgraded MPI GEOS-3 operational system, with improved computational performance, provided daily first-look and late-look assimilation data products to EOS instrument teams. In July 2002, this upgraded system was used to begin the production of a unique multiyear GEOS-3 TRMM reanalysis incorporating TRMM and SSM/I tropical precipitation data from November 1997, and onwards.

The implementation of the GEOS-4 operational system was successfully completed. The data assimilation engine in the GEOS-4 system is fvDAS, the DAO next-generation data assimilation system. The DAO worked closely with EOS Instrument Teams, DAO data users, and external elements, such as the ECS and DAAC, to define the new interfaces for the GEOS-4 products and to coordinate the implementation schedules and system test planning. The DAO has started working with the Aura Instrument Teams (MLS, TES, HIRDLS, and OMI) to define data and operational requirements in preparation for the Aura launch. The DAO completed both the stand-alone tests of GEOS-4 data at user sites and the end-to-end data flow test with no significant discrepancies encountered. The GEOS-4 data products file specification incorporates all the critical user feedback collected during the user review cycle. The GEOS-4 system commenced operations with data from October 1, 2002. GEOS-3 operations stopped at the end of October 2002. The DAO also started the Reanalysis for the Stratospheric Trace gas Study (ReSTS) using the GEOS-4 system. The data period planned for ReSTS is 1991 through 1995. The GEOS-4 reprocessing in support of MODIS, spanning the whole EOS/Terra period with a fixed system, started in late October 2002.

In April 2002, the SAGE III project joined as a new operational user of the GEOS DAS data products. SAGE III uses temperature profile information in the GEOS first-look data products to support validation efforts during field campaigns and to aid in instrument performance evaluation.

2. DAO research pursuing innovative ways to assimilate TRMM and SSM/I precipitation measurements has highlighted NASA's role in the U.S. Weather Research Program (USWRP) by providing observations from space that have the potential of significantly improving operational hurricane track and landfall predictions to mitigate human and economic losses. Results showed that GEOS analyses incorporating microwave-based satellite rainfall data yielded better track predictions for Hurricanes Bonnie and Floyd, and notably higher scores for quantitative precipitation forecasts up to 5 days.

3. The DAO has tested and evaluated a number of new observation types in the context of fvDAS, namely wind observations from the EOS MODIS and MISR instruments, and in situ wind observations obtained on board commercial aircraft (GADS). Initial tests with the MODIS winds were highly promising, and important feedback on data quality to the GADS and MISR teams have been obtained from assimilation experiments using these data. A comprehensive set of Observing System Experiments (OSEs) has been carried out in order to apportion the respective contributions between the various components of the observing system. The satellite

data were shown to be crucial to the performance in the Southern Hemisphere, but recent versions of fvDAS have shown a much stronger sensitivity to satellite data in both hemispheres.

Two examples are given of the science activities of the DAO in the following short articles. The first is on the assimilation and validation of ozone data by Ivanka Stajner; the second is on Observing System Experiments by Robert Atlas.

Ozone Assimilation: Validation in the Tropical Troposphere

Ivanka Stajner (istajner@dao.gsfc.nasa.gov)

An ozone data assimilation system at the Data Assimilation Office (DAO) provides global ozone fields. This system is being used in preparation for EOS Aura with a series of experiments investigating the use of column ozone from either TOMS or SBUV, and vertical ozone profiles from SBUV. Initial application of the system and its design have been focused on stratospheric ozone.

Here we show the sensitivities of the assimilated ozone to the total column ozone data source and to the meteorological atmospheric assimilation system that provides the winds. Validation is focused on tropical ozone and uses the Southern Hemisphere ADditional Ozonesondes (SHADOZ) measurements from 1998. Figure 5-1 shows that the annual mean of the assimilation using SBUV total column (blue) is in better agreement with SHADOZ sondes (black) than the assimilation using TOMS total ozone column data (green). Even though the assimilated ozone remains high biased in the lower stratosphere and troposphere, the shape of the profile is improved with the capture of the characteristic “S” shape. The shape is further improved with the use of winds from a newer (GEOS-4) data assimilation system, which includes the DAO’s finite volume general circulation model (red curve in Figure 5-1). Figure 5-2 illustrates good agreement in the temporal variability of the sonde and assimilated profiles in a region controlled by the dynamical variability. Lower ozone values are seen in the first half of the year, and highest values are in September and October. Vertical extent and altitude of many anomalies are captured well. For example, a profile on October 30 shows two positive anomalies: around 300 and 700 hPa. These anomalies are captured in the assimilation, despite the lack of information about the shape of the tropospheric profile from the SBUV and TOMS data that were used in the assimilation.

The upcoming online implementation of the transport that will include convection, and the incorporation of the Harvard parameterized chemistry in the troposphere, are expected to reduce the bias and capture the temporal variability caused by the pollutants.

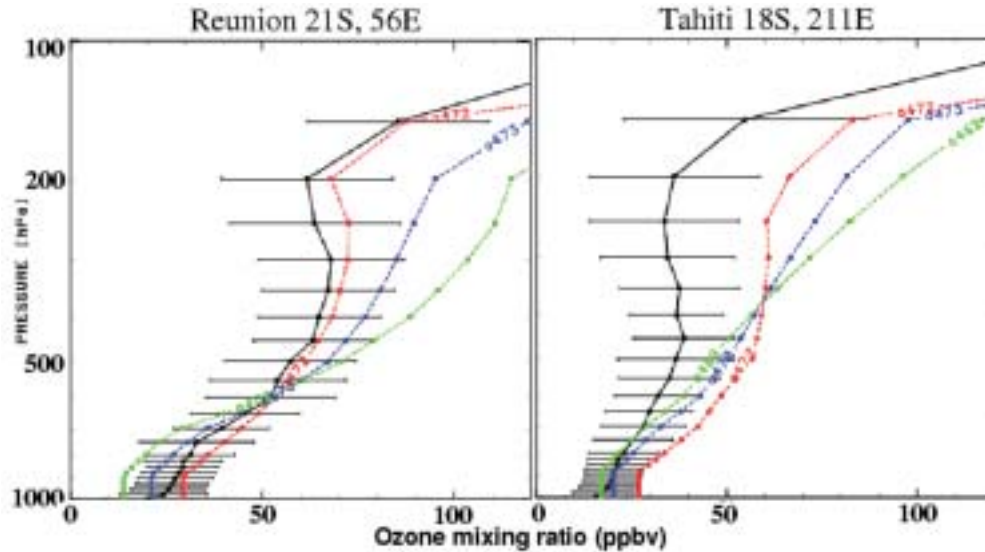


Figure 5-1. Three ozone assimilation experiments are compared with independent SHADOZ ozone sondes using annual mean of the profiles collocated with sondes. Assimilation using SBUV total column (blue) is in better agreement with SHADOZ sondes than the assimilation using TOMS total column (green). Transport in both these experiments used GEOS-2 winds. The shape of the assimilated profile improves further with the use of GEOS-4 winds in the transport (red). Note that the last experiment captures the characteristic "S" shape in the profile with relatively low ozone values around 250 hPa. The length of a black horizontal line denotes the size of the standard deviation of the sonde measurements at each pressure level in the annual time series.

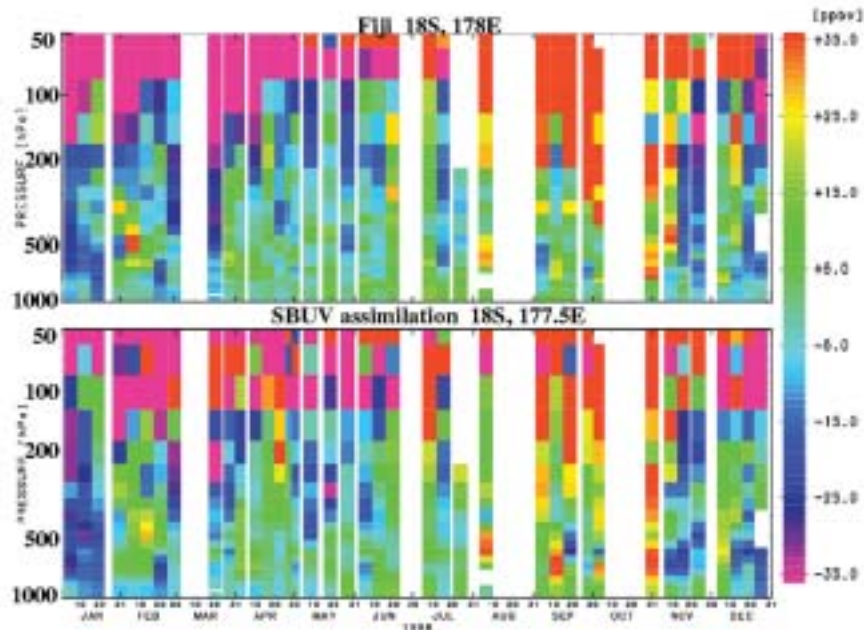


Figure 5-2. Time series of ozone anomalies are shown: for the independent sonde measurements in the upper panel, and for the ozone assimilation in the lower panel.

Observing System Simulation Experiments

Robert M. Atlas (Robert.M.Atlas@nasa.gov)

Since the advent of meteorological satellites in the 1960's, numerous experiments have been conducted in order to evaluate the impact of these and other data on atmospheric analysis and prediction. Such studies have included both OSEs (Observing System Experiments) and OSSEs (Observing System Simulation Experiments). The OSEs were conducted to evaluate the impact of specific observations or classes of observations on analyses and forecasts. Such experiments have been performed for selected types of conventional data and for various satellite data sets as they became available. The OSSEs were conducted to evaluate the potential for future observing systems to improve Numerical Weather Prediction (NWP) and to plan for the Global Weather Experiment and more recently for EOS. In addition, OSSEs have been run to evaluate trade-offs in the design of observing systems and observing networks, and to test new methodology for data assimilation.

OSSEs are currently being conducted at the NASA Data Assimilation Office (DAO) in order to determine the potential impact of space-based lidar wind profiles in current data assimilation/numerical weather prediction systems and to evaluate tradeoffs in lidar instrument design. In the first of these experiments, the nature run (reference atmosphere) was generated using an early version of the Finite Volume General Circulation Model (fvGCM) at .5 degree resolution, and the assimilation and forecast system was the current operational version of the GEOS 3 Data Assimilation System at 1 degree resolution. This nature run is substantially longer than earlier nature runs and covers a three-and-one-half month period. In addition, the nature run contains very interesting and important meteorological features, including tropical cyclones and very realistic representations of atmospheric fronts and extratropical cyclone evolution.

Following a very detailed assessment of the realism of the nature run and the differences between the nature run model and the assimilation/forecasting model, the entire OSSE system was validated through a comparison of parallel real data and simulated data impact experiments. Then parallel assimilation experiments and 14 five-day forecasts were performed with this system to evaluate the impact of idealized space-based lidar wind profiles. As in earlier OSSEs (Atlas, 1997, Lord et al., 2001), one of the major metrics for assessing the potential impact of lidar winds was the anomaly correlation for sea level pressure and 500 mb height forecasts. In addition, a number of additional metrics, such as impact on the central pressure and displacement of cyclones or the landfall of hurricanes was also evaluated.

The results of this evaluation showed a very substantial improvement in forecast accuracy resulting from the assimilation space-based lidar winds. In the Southern Hemisphere, average forecast skill was extended by 12–18 hours, while in the Northern Hemisphere, average forecast skill was extended by 3–6 hours. This was associated with a meaningful (10%) reduction in position error for all cyclones averaged over the globe and all time periods. For very intense cyclones (those with central pressure less than 945 hPa), the reduction of position error exceeded 200 km. A meaningful impact on the prediction of hurricane landfall is shown in Figure 5-3, which illustrates the improvement in hurricane landfall prediction as a result of assimilating wind lidar data. This result was obtained for the first hurricane in the nature run. The predicted landfall position error for the two tropical cyclones to hit the U.S. mainland in the nature run was improved by approximately 150 miles for both storms. These results demonstrate considerable potential for space-based lidar wind profile measurements; however, further experiments are needed to evaluate the specific characteristics of proposed lidars.

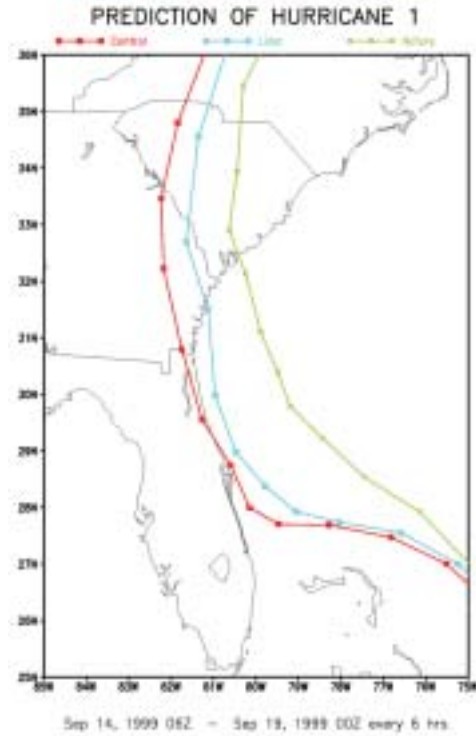


Figure 5-3. Potential impact of new space-based observations on Hurricane Track Prediction based on OSSEs at NASA Data Assimilation Office. Tracks: green is the actual track; red is the forecast beginning 63 hours before landfall with current data; and blue is the improved forecast for the same time period with simulated wind lidar. The dollar savings is ~ \$1M/mile per hurricane for improved landfall forecast. Thus the wind lidar in this one case reduces landfall prediction error by 66% and would potentially save > \$165M.

Mesoscale Atmospheric Processes Branch, Code 912

Branch Summary

The Mesoscale Atmospheric Processes Branch seeks to understand the contributions of mesoscale atmospheric processes to the global climate system. Research is conducted on the physical and dynamical properties, structure and evolution of meteorological phenomena ranging from synoptic scale down to micro scales, with a strong focus on the initiation, development and effects of cloud systems. A major emphasis is placed on understanding energy exchange and conversion mechanisms, especially cloud microphysical development and latent heat release associated with atmospheric motions. The research is inherently focused on defining the atmospheric component of the global hydrologic cycle, especially precipitation, and its interaction with other components of the Earth system. Branch members participate in satellite missions and develop advanced remote-sensing technology with strengths in the active remote sensing of aerosols, water vapor, winds, and convective and cirrus clouds. There are also strong research activities in cloud system modeling, and in the analysis, application and visualization of a great variety of data.

1) Branch scientists develop retrieval techniques to estimate precipitation using satellite observations from the Tropical Rainfall Measurement Mission (TRMM) and other satellites such as GOES and the new AMSR-E sensor on EOS Aqua. The accompanying article on TRMM describes recent accomplishments including new 3-hourly rainfall fields in near real time, development of a new effective El Niño predictor, and application of TRMM data to study of the urban heat island effect. The TRMM Ground Validation team processes and applies data from rain gauge networks, and ground-based radars. TRMM and other precipitation data are used within the branch for a wide spectrum of studies on precipitating cloud systems and global water cycle. Increasingly, these activities integrate global or regional data sets with modeling. Research is conducted on the assimilation of TRMM observations into models to explore the potential benefits to weather forecasting, such as for hurricanes, and to improve understanding of precipitating cloud systems. Branch scientists are also an integral part of the developing Global Precipitation Measurement (GPM) mission, presently in formulation phase. GPM seeks to establish an international calibrated satellite network for high-resolution (space and time) global precipitation measurements.

2) Development of *lidar technology* and *application of lidar data* for atmospheric measurements are also key areas of research. Systems have been developed to characterize the vertical profile structure of cloud systems (Cloud Physics Lidar–CPL), atmospheric aerosols (Micro-Pulse Lidar–MPL), water vapor (Scanning Raman Lidar–SRL) and winds (Goddard Lidar Observatory for Winds–GLOW) at fine temporal and/or spatial resolution from ground-based, airborne and satellite platforms. In addition, the Cloud Radar System (CRS), a new millimeter-wavelength radar for profiling cloud systems has been developed and integrated on NASA’s high-altitude ER-2 research aircraft for use in sensing the microphysical properties of cirrus and other cloud types, and complements the existing ER-2 Doppler (EDOP) radar that has been extensively used to study precipitating cloud systems.

The ground-based SRL, GLOW and HARLIE systems participated in the International H₂O Project (IHOP) in May–June 2002. The CPL, CRS and EDOP were all deployed on NASA’s ER-2 aircraft for the Cirrus Regional Study of Tropical Anvils and Cirrus Layers-Florida Area Cirrus Experiment (CRYSTAL-FACE) in July 2002. More detailed descriptions of the participation of branch scientists and observing systems in these major field experiments may be found in the following IHOP and CRYSTAL-FACE highlights.

Branch scientists developed atmosphere-sensing capabilities of the Geoscience Laser Altimeter System (GLAS) system that was launched on ICESat early in 2003. The GLAS will be used to profile the vertical distributions of cloud and aerosol layers. Branch scientists also serve as Project Scientists for the Earth System Science Pathfinder (ESSP) CALIPSO (lidar) and CloudSat (mm-radar) missions that are planned for launch in 2004.

The Micro-Pulse Lidar Network (MPLNET) is comprised of ground-based MPL systems, co-located with sun/sky photometer sites in the NASA Aerosol Robotic Network (AERONET). MPLNET data, together with the co-located AERONET results, provides information on aerosol and cloud vertical structure, optical depth, particle size and shape, aerosol absorption, and sky radiance. Notable accomplishments for 2002 include publication of data processing algorithms and papers derived from observations taken during INDOEX-99, ARREX, and SAFARI-2000. In addition, MPL systems were deployed in support of CRYSTAL-FACE and the Brazil-based Smoke Aerosols, Clouds, Rainfall and Climate (SMOCC) experiment during the past year. MPLNET observations have also proven very useful for modeling GLAS algorithm performance and accuracy. MPLNET data products are documented and available to the scientific community via the project Web site (<http://mplnet.gsfc.nasa.gov>).

3) Cloud-resolving (Goddard Cumulus Ensemble, GCE) and mesoscale (MM5) models are used in investigations of the dynamic and thermodynamic processes associated with tropical and extratropical cyclones and rainbands, and tropical and mid-latitude deep convective systems. The models are also used to research cloud-chemistry interactions, stratospheric-tropospheric interactions, and the effects of the ocean surface (sea surface temperature) and land surface (vegetation and soil moisture) on atmospheric convection and weather systems. Other important applications include assessment of the potential benefits of assimilating satellite-derived water vapor and precipitation fields on simulations and forecasting of tropical and extra-tropical regional-scale weather systems (i.e., hurricanes, and cyclones). Long-term integrations of the models are used to investigate climate feedback mechanisms, such as cloud-radiation interactions. The simulations provide a basis for integrated systemwide assessment of important factors such as surface energy and radiative exchange processes, and diabatic heating and water budgets associated with tropical and mid-latitude weather systems. The models are also used to develop retrieval algorithms. For example, the GCE model is providing TRMM investigators with four-dimensional data sets for developing and improving TRMM rainfall and latent heating retrieval algorithms. The scientific output of the modeling activities was again exceptional in 2002 with 15 new papers published and many more submitted. Further details can be found in the accompanying GCE Model article.

Branch scientists have active participation and leadership in various international model comparison and evaluation activities of the GEWEX Cloud System Study for the purpose of increasing confidence in the cloud-resolving models and facilitating research on the development and testing of cloud parameterizations used in large-scale climate and forecast models (GCMs). Of particular note is a model comparison study of microphysical development in cirrus clouds that identifies key parameters, such as deposition coefficient, to which the models are highly sensitive and for which additional information is required (e.g., laboratory studies).

4) The Branch has developed a world-class visualization lab that is being increasingly used in high profile settings to reach out to scientists and, very importantly, to citizens and Government organizations to stimulate understanding and support of NASA's Earth Science Enterprise and its missions. The TRMM Outreach Office, Earth Observing System (EOS) Project Science Office, Earth Sciences Directorate and NASA Earth Science Enterprise (HQ) heavily utilize these capabilities in bringing the value of NASA missions and science accomplishments to the forefront of U.S. Global Change Research.

Tropical Rainfall Measurement Mission (TRMM)

Jeffrey Halverson (halverson@agnes.gsfc.nasa.gov)

Now in its fifth year since launch, NASA and NASDA's Tropical Rainfall Measurement Mission (TRMM) satellite continues to collect a variety of measurements designed to answer an array of climate and weather questions related to Earth's water cycle. The primary objectives are to provide distributions of rainfall and latent heating in the tropics, understand how tropical rainfall influences the global circulation, improve the initializa-

tion of 24-hour to short-range climate forecasts, and diagnose and predict the development of climate-varying phenomenon like the El Niño Southern Oscillation (ENSO).

One of the great achievements of the TRMM program is the breadth of its science, and the diversity of its potential societal applications. In 2002, scientists in the Mesoscale Atmospheric Processes Branch (Code 912) continued to be active in virtually every component of the TRMM program, including algorithm development, research analysis, ground validation, educational outreach, and transfer to societal applications.

Branch scientists, led by Robert Adler and George Huffman, continue to develop algorithms in support of the TRMM mission. A multisatellite, near real-time, 3-hourly rainfall product has been developed using a combination of TRMM, polar orbit microwave, and geosynchronous infrared (IR) data. The product is available at the TRMM Web site (<http://trmm.gsfc.nasa.gov>) and has shown skill at accurately retrieving rainfall totals associated with extreme weather events. In addition, Scott Curtis and Robert Adler have developed an ENSO precipitation index (ESPI) using TRMM satellite estimates to predict the onset of the El Niño/La Niña cycle. Large values of the ESPI occur when rapid fluctuations in the Indian Ocean precipitation gradient (and accompanying westerly wind bursts) drive the ocean towards an El Niño state (Figure 5-4a). On February 7, 2002, an El Niño was predicted to begin between July and October 2002 (as seen by a rapid increase in ESPI in Figure 5-4a). At the same time other institutions produced forecast-probabilities of ~ 50%. Figure 5-4b shows the validation of the 2002 El Niño forecast with the conventional Niño 3.4 index.

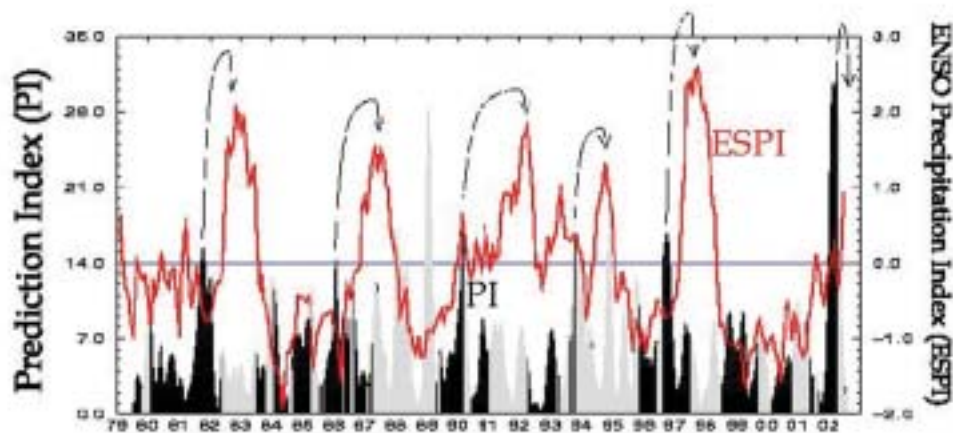


Figure 5-4a. ENSO Precipitation index.

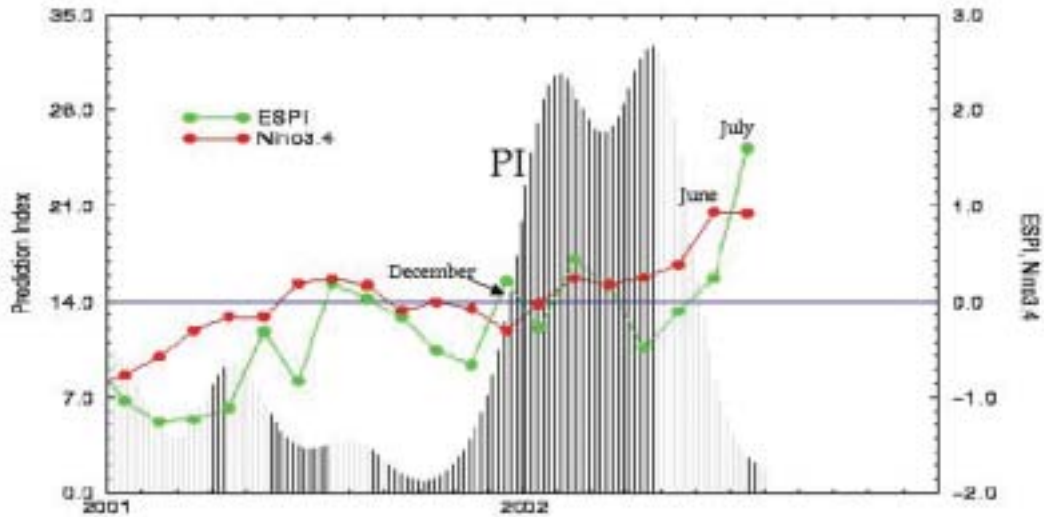


Figure 5-4b. 2002 ESPI prediction.

Wei-Kuo Tao and colleagues continue to progress towards the first generation of latent heating algorithms. Tao’s group uses TRMM precipitation radar and the Goddard Convective-Stratiform Heating (CSH) algorithm to retrieve latent heating values at different atmospheric levels. Wei-Kuo Tao’s cloud model work is a critical component of TRMM’s latent heating retrieval and microphysical validation efforts.

Marshall Shepherd and colleagues used data from the TRMM precipitation radar to identify rainfall anomalies downwind of cities (Shepherd et al. 2002). It is hypothesized that urban land use/change impacts convective processes that produce rainfall. Recent work by Shepherd and Steve Burian (University of Arkansas) identified rainfall anomalies over and downwind of Houston, Texas, (Figure 5-5) that correspond to recently published lightning anomalies (Orville et al. 2001). NASA funding has been received to extend this work to other cities and incorporate coupled land-atmosphere models.

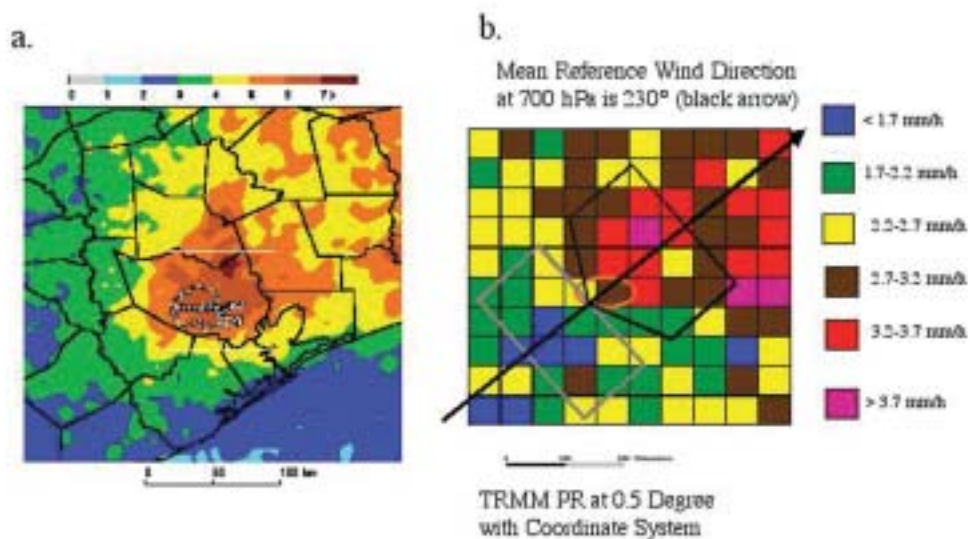


Figure 5-5. Rainfall from TRMM, 5-5a, and lightning anomalies, 5-5b, (Orville et al., 2001) over and downwind of Houston Texas. Orange oval is the central Houston urban district.

International H₂O Project (IHOP-2002)

Belay B. Demoz (Belay.B.Demoz@nasa.gov)

Accurate forecasting of the rainfall in the summer months is difficult. This limitation has important consequences to society. As an example, flash floods, which may result from heavy rainfall in a very localized area, are responsible for more deaths than hurricanes, tornadoes, windstorms, or lightning. Atmospheric moisture is a key ingredient for convective precipitation and there have been significant improvements in measurement capability over the last decade. The International H₂O Project (IHOP-2002) was a major field experiment conducted in May–June 2002 over the southern Great Plains to explore the possible improvements in forecasting convective precipitation that could result from improved water vapor measurements and their incorporation in forecast models. Members of the Mesoscale Atmospheric Processes Branch were key participants in IHOP-2002, which involved a diverse collection of scientists from universities, NOAA, DOE, and other organizations. Integration of the observations with models is fundamental to the IHOP-2002 strategy.

IHOP-2002 was comprised of four main research foci: Quantitative Precipitation Forecasting (QPF), Convection Initiation (CI), Atmospheric Boundary Layer (ABL), and Instrumentation. Under QPF, IHOP will determine if better humidity measurements improve the performance of weather forecast models for rainfall prediction. IHOP will also assess if humidity and wind measurements can help in forecasting the timing and location of new storms (CI). A key concern is the relationship between land surface variations and air moisture variations (ABL). Humidity is a difficult quantity to measure, and a combination of instruments may be needed to obtain the most useful set of measurements. Determining the best combination of humidity-measuring instruments to better predict rainfall amounts is being addressed under Instrumentation. Central to understanding convective precipitation in this region is the dryline phenomena. Characterizing the dryline and its evolution is integral to IHOP-2002.

The Scanning Raman Lidar (SRL), the Holographic Airborne Rotating Lidar Instrument Experiment (HARLIE) and the Goddard Mobile Lidar Observatory for Wind (GLOW) were deployed for IHOP-2002. SRL provided profiles of water vapor mixing ratio to reveal the water vapor stratification to altitudes of 10 km or more. HARLIE provided data characterizing ABL structure and winds. GLOW provided measurements of wind speed and direction from the surface into the stratosphere. All these active remote-sensing measurements have excellent vertical and temporal resolution and provide a vastly more detailed picture than conventional observations.

The lidars were co-located at a remote ground site in the western panhandle of Oklahoma together with the NCAR S-Pol radar, profilers, sodars (sound detection and ranging), and many other instruments. This location is highly favored for airmass convergence and drylines.

One of the objectives is to examine the link between ABL processes, water vapor, wind and convection. An example of data that would allow us to accomplish this is shown in Figures 5-6a,b,c. It shows the evolution of a dryline over our site on 22 May 2002. The dryline was better defined after sunset (0025 UTC) compared to its daytime structure, which is modified by the convectively active boundary layer. The vertical mixing by the updraft plumes caused by surface heating, together with the terrain slope in this area, is hypothesized as the cause for an apparent eastward movement of the dryline after sunrise. We plan to quantify this mesoscale variability and test the theory. Characterization of these updraft plumes is also important in convective initiation modeling. Cumulus clouds form on top of updraft columns, which can be seen best from the HARLIE measurements. If these clouds are to be correctly modeled, one needs to know the profile of moisture within the updraft plumes. We are in the process of identifying and analyzing updraft plumes using HARLIE, SRL and other instruments that were co-located at our site, like the University of Massachusetts Frequency Modulated Continuous Wave (FMCW) radar, NCAR Integrated Sounding System (ISS), Multiple Antenna Profiling Radar (MAPR), S-Pol radar, and many others.

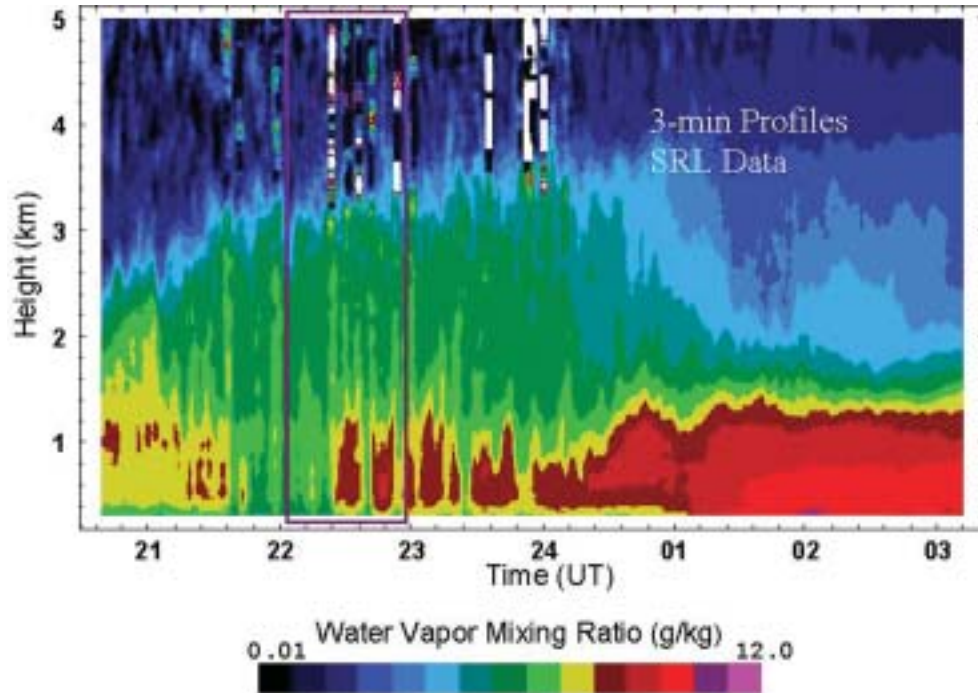


Figure 5-6a. Time-height plot of the Scanning Raman lidar measured water vapor mixing ratio for the 22 May 2002 dryline case at Homestead, Oklahoma. It shows cloud locations (vertical white strips), evolution of the water vapor mixing ratio and hence the dryline, day and nighttime characteristics of the boundary layer, and the well-defined contours of the dry line boundary in late afternoon and after sunset (0025 UTC).

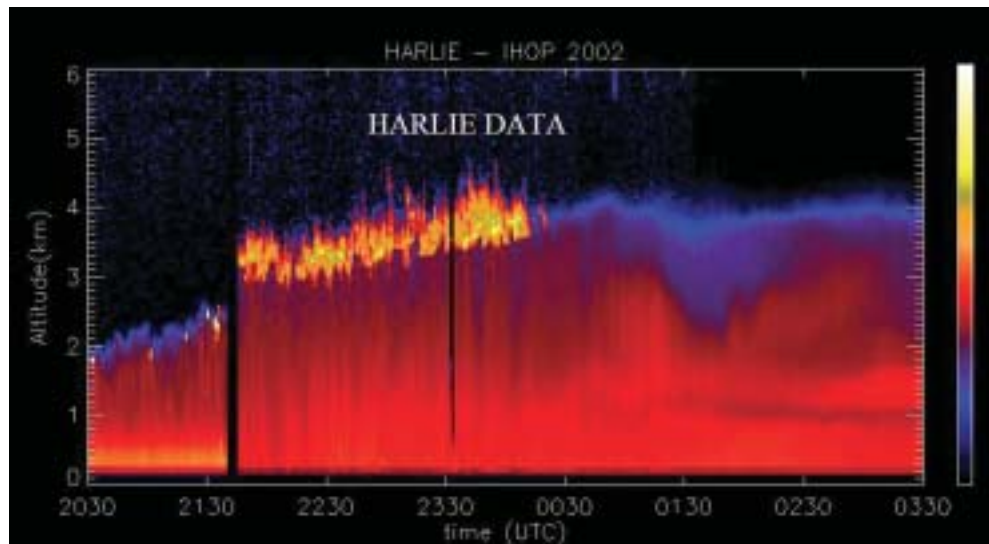


Figure 5-6b. Time-height plot of the HARLIE-measured aerosol backscatter profile data for the 22 May 2002 dryline case at Homestead, Oklahoma. The daily evolution of the atmospheric boundary layer (formation in the daytime and its demise after sunset, at about 0100 UTC) and location of cumulus clouds present is revealed. The gap near 2130 is data lost due to time delay in switching between modes of operation, from staring at an angle to conical scan. The profiles shown in the figure after this gap are averages of every 360-scan, leading to an apparently continuous cloud deck. Note that the day-night transition in the HARLIE and the SRL data reveal the sudden decrease in BL height and no cumulus clouds after the Sun sets—a manifestation of the absence of the surface forcing.

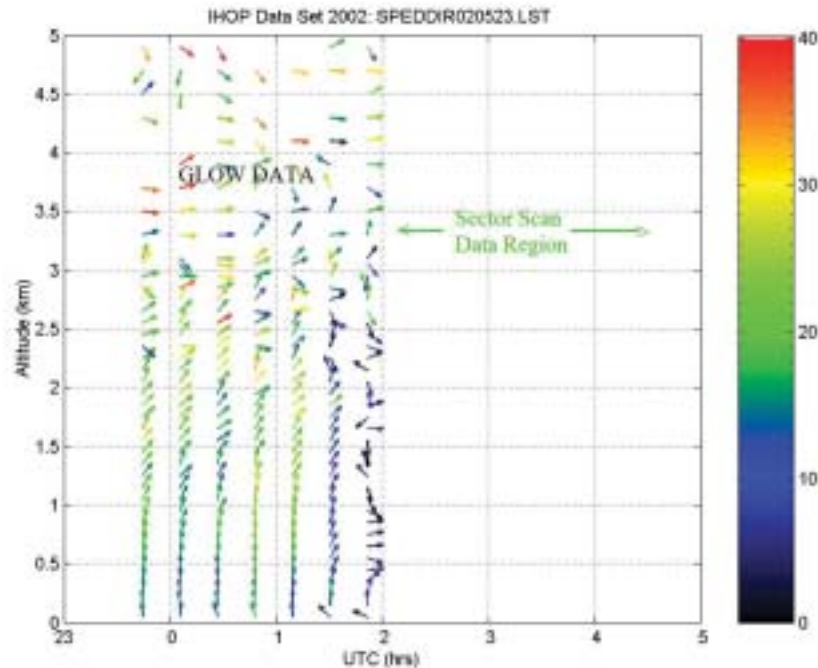


Figure 5-6c. Time-height plot of the GLOW-measured wind speed and direction for the 22 May 2002 dryline case at Homestead, Oklahoma. Low-level wind shifts associated with the dryline are noticeable. This information will be integrated with data from the other sensors to describe the complete evolution of the dryline. These data sets will also be augmented with vertical wind and other data of ABL properties for the Homestead site. Location of the updrafts will be determined from the radars (e.g., the FMCW) and mapped to the wind, aerosol backscatter and moisture observations to determine the mesoscale and convective scale ABL variability.

Goddard Cumulus Ensemble (GCE) Model

Wei-Kuo Tao (Wei-Kuo.Tao-1@nasa.gov)

The Goddard Cumulus Ensemble (GCE) model, a 3-dimensional model that explicitly resolves cloud and mesoscale processes, was used to simulate convection that occurred during the TRMM LBA field experiment in Brazil. Convection in this region can be categorized into two different regimes: low-level *easterly* or low-level *westerly* flow. Low-level easterly flow results in moderate to large CAPE (convective available potential energy) and a relatively dry environment. The resulting convection is more intense, like that seen over mid-latitude continents. Conversely, low-level westerly flow results in smaller CAPE and a moist environment. Convection is weaker and more widespread, similar to oceanic or monsoon-like systems. The GCE model was recently used to study both regimes in order to provide cloud data sets representative of both environments in support of TRMM rainfall and heating algorithm development. Two different cases were examined: January 26, 1999, an easterly regime case, and February 23, 1999, a westerly regime case. The January 26 case is an organized squall line and the February 23 case is less organized with only transient lines. The results show latent heating distributed over a deeper layer with a less pronounced peak for the January 26 easterly regime case. Also, reinforced is the notion that ice processes are more important in this regime, consistent with the observed electrical activity. Figure 5-7 shows the observations (provided by Drs. S. Rutledge and R. Cifelli/CSU) and the 3-D GCE model results. In addition, the GCE model has been linked to a passive radiative transfer model developed by C. Kummerow (CSU) to utilize satellite data in order to modify and improve the “cloud microphysics” used in cloud-resolving models as shown in Figure 5-8.

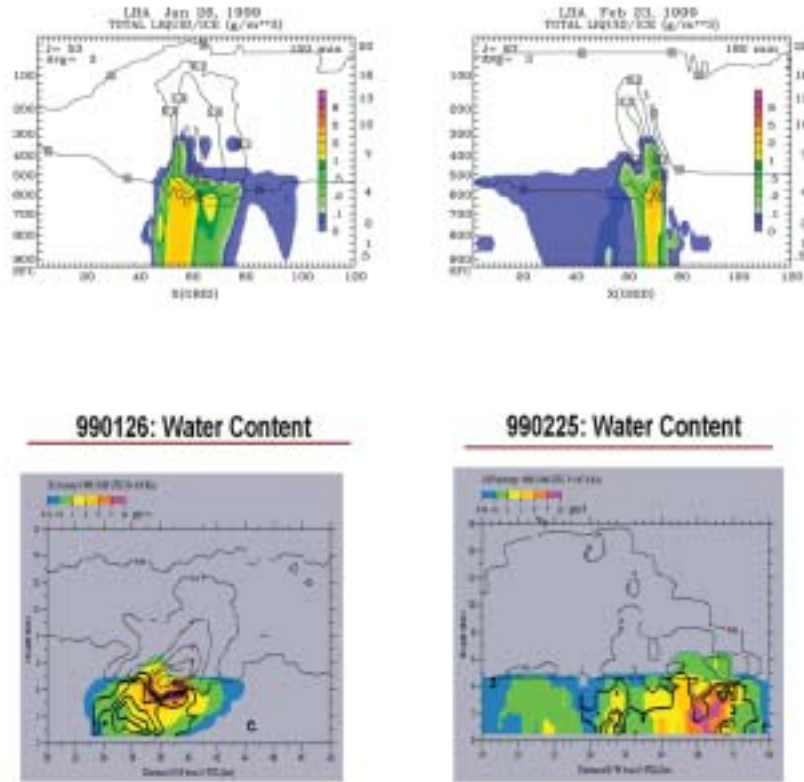


Figure 5-7. Liquid and ice water contents (g m^{-3}) for cases typical of two different convective regimes from radar observations (top) and 3-D GCM model simulations (bottom) for January 26 (left) and February 23/25 (right) during TRMM LBA in 1999. The January case is an easterly flow regime while the February cases are a westerly regime. Note the differences in organization and scale of the convective cores, as well as in the extent of the stratiform precipitation regions, which are well captured by the model. Radar analysis courtesy of S. Rutledge and R. Cifelli of Colorado State University.

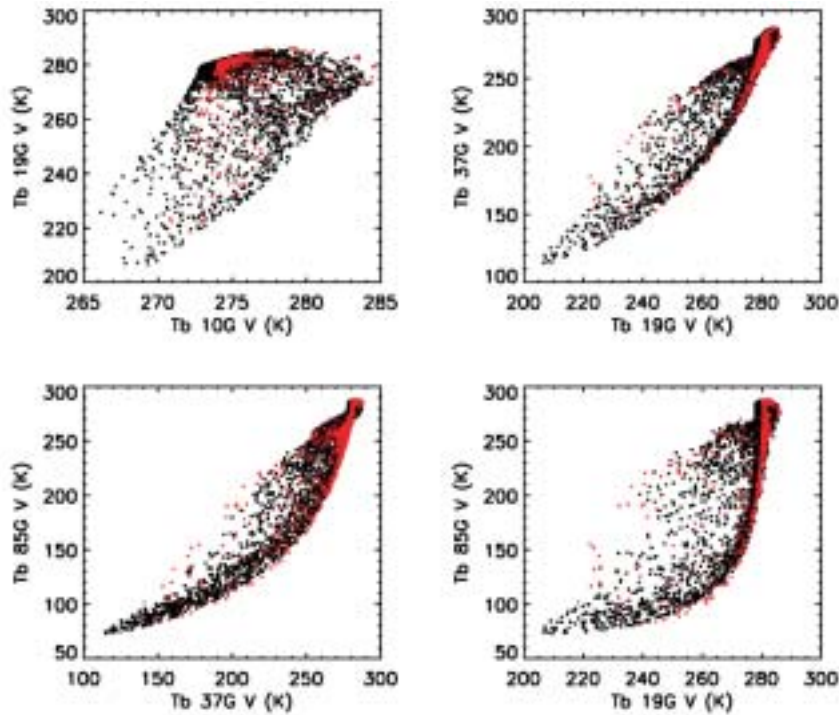


Figure 5-8. Simulated brightness temperature scatter plots at different TMI channels using GCE model outputs. Black squares are January 26, 1999, case and red squares are February 23, 1999, LBA case. January 26 case has stronger convection and more ice.

Of the main types of extratropical cyclone-related mesoscale rainbands, the most intense rainfall rates are usually associated with Narrow Cold Frontal Rainbands (NCFRs). A NOAA P-3 instrumented aircraft observed an intense, fast-moving NCFR as it approached the Pacific Northwest coast on 19 February 2001 during the Pacific Coastal Jets Experiment. The NCFR produced hail along the California coast when it made landfall. An outstanding feature of the NCFR was the breaks (gaps) observed along the rainband by Doppler Radar. A mesoscale model, MM5, was used to simulate this NCFR. The numerical simulations were conducted using nested grids with resolutions of 36 km, 12 km, 4 km and 1.3 km. The high-resolution domain was able to reproduce the main structural features of the observed NCFR Figure 5-9 (provided by Dr. D. Jorgensen/NOAA). The breaks (gaps) along the rainband are well represented. Based on the simulated results, many aspects of NCFR structure depicted in previous studies were confirmed.

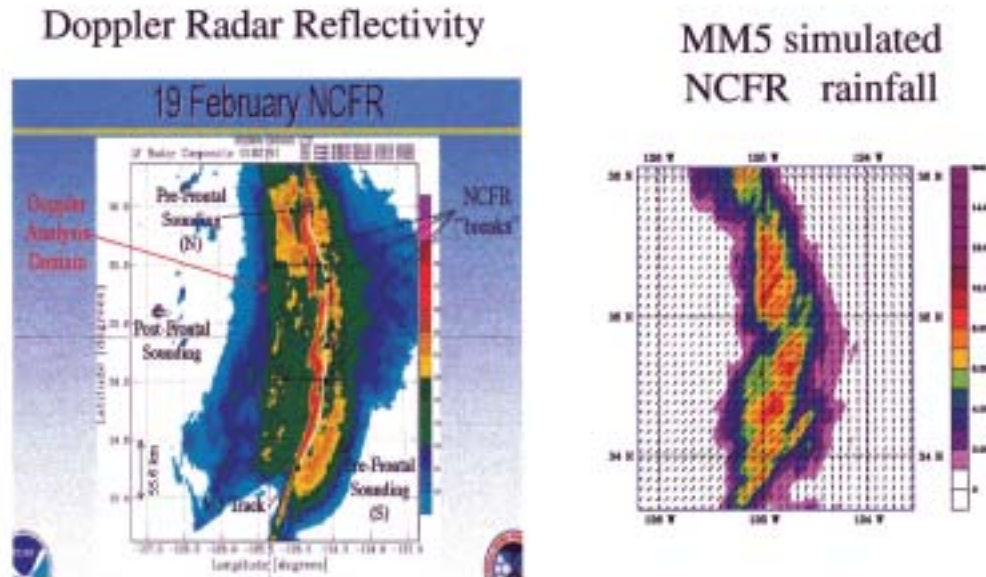


Figure 5-9. MM-5 simulation (right) of precipitation field for Narrow Cold Frontal Rainband (NCFR) observed (left) on February 19 during PACJET 2001. The simulations were conducted with nested grids of 36, 12, 4 and 1.3 km. With the high-resolution inner domain, the simulation reproduced the main structural features of the NCFR. The breaks (gaps) in the rainband were well represented. The results of this study confirmed many aspects of NCFR structure described in prior studies.

In addition, regional scale model experiments were conducted to quantify the water cycle over the South China Sea and its impact on mid-latitude water vapor transport during different climate regimes (1997 and 1998). We also conducted cloud-resolving (process) model simulations of convective systems that developed over different geographic locations (i.e., S. China Sea, W. Pacific, E. Atlantic, and central U.S.) to provide a better understanding of the precipitation efficiency and surface energy budget, and their system-to-system differences.

CRYSTAL-FACE

David O'C Starr (David.O.Starr@nasa.gov)



Members of the Laboratory for Atmospheres played key roles in the Cirrus Regional Study of Tropical Anvils and Layers-Florida Area Cirrus Experiment (CRYSTAL-FACE), a major NASA field experiment conducted in south Florida in July 2002. The experiment sought to:

- 1) Improve understanding of cirrus anvil properties in relationship to the properties and strength of deep convection.
Does stronger convection imply a larger longer-lived anvil; more anvil ice mass; larger ice crystals; more complex ice crystals?
- 2) Provide a direct basis for improvement of large-scale models used for numerical weather prediction and climate studies by quantitatively linking anvil properties to convective mass flux, a parameter predicted in such models.
- 3) Improve understanding of the physical factors that control lifetime and area coverage of cirrus anvils and tropical cirrus layers.
What are the roles of microphysical, radiative and dynamical processes in cirrus cloud development and lifecycle and what are the effects of environmental factors such as humidity and stability?
- 4) Improve understanding of how deep convection affects tropical upper tropospheric and lower stratospheric humidity, a key climate-radiation variable, and also a key factor in stratospheric chemistry.

These objectives support the evaluation and improvement of state-of-the-art, high-resolution, cloud system models that account for the full range of cloud physical processes and provide another path for improvement of global circulation models (GCMs).

An additional objective was the validation of ground-based and satellite remote sensing observations of cloud properties including observations from Terra (MODIS, MISR, CERES), Aqua (MODIS, AIRS, CERES), GOES, POES, and TRMM (Precipitation Radar) as well as to provide data sets supporting algorithm development for future measurements from space such as lidar (CALIPSO) and millimeter wavelength radar (CloudSat)—key elements of NASA's "A-Train" that will be in place in 2004.

CRYSTAL-FACE was principally sponsored by NASA under the Code Y Radiation Sciences Program, the Upper Atmosphere Research Program, the EOS Validation Program, and the Atmospheric Chemistry Modeling and Analysis Program. Additionally, CRYSTAL-FACE was also sponsored by the National Science Foundation, the Department of Energy Atmospheric Radiation Program (ARM), the Office of Naval Research, and the NASA-NOAA-DOD Integrated Program Office. The National Weather Service (NOAA) was a cooperating agency.

There were six aircraft participating in CRYSTAL-FACE: NASA's ER-2 and WB-57, the Proteus (contracted by IPO), the University of North Dakota Citation, Naval Research Laboratory's P-3 and CIRPAS Twin Otter, as shown on the cover of this report. The aircraft were based at Key West Naval Air Facility where the science team of over 200 members was assembled.

There were two cloud-observing ground sites, located at Tamiami Airport, near Miami, and at Everglade City on the west coast of southern Florida. Goddard provided and staffed the Surface Measurements for Atmospheric Radiative Transfer (SMART, Tsay/913) system at the eastern site that included a Micropulse Lidar (MPL, Welton/912) and a suite of radiometers. In addition, a sophisticated polarimetric precipitation radar (Goddard's NPOL radar from Wallops Flight Facility, Gerlach/972) was operated at Ochopee, 5 km east of Everglades City. In-flight aircraft operations were directed from this location, Figure 5-10. Multi-aircraft science missions were conducted on 12 days with the ER-2 flying 11 missions. Underflights of Terra (3) and Aqua (5) were performed and good coordination was often achieved with the ground sites. On many occasions, all six aircraft flew simultaneous coordinated patterns.



Figure 5-10. (Left) David Starr/912 (back) and ex-ER-2 pilot Jan Nyström direct CRYSTAL-FACE aircraft operations from the NPOL site. Also shown are Paul Cucera of University of North Dakota and John Gerlack/972 at Ochopee using real-time displays of GOES imagery (provided by team at NASA LaRC), NPOL and NWS NEXRAD data, FAA flight-tracking data, and information from the ground sites. (Right) NPOL site at Ochopee, Florida. Photos courtesy of Ed Zipser, University of Utah.

Goddard investigators played key roles in the successful execution of the mission, serving as ER-2 Platform Scientist (Platnick/913, King/900, Newman/916) and as the co-Mission Scientist responsible for real-time direction of in-flight aircraft operations (Starr/912). In addition, daily regional forecasts of convective activity and chemical transport (Figure 5-11) were generated to support mission planning using MM5 (Wang/JCET/912 and Pickering/ESSIC/916). Other 910 scientists supported the daily mission planning cycle in various ways.

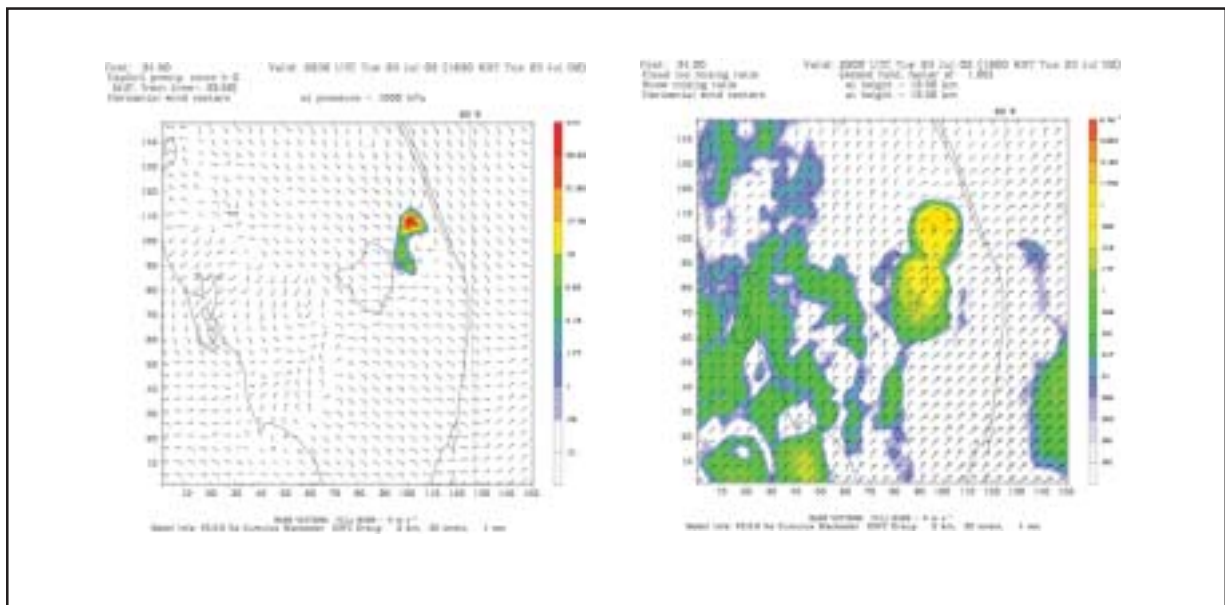


Figure 5-11. Forecasts using nested MM5 for CRYSTAL-FACE on July 23, 2002. Shown are examples of (left) precipitation and low-level wind fields; and (right) upper level cloud mass and winds at 2200 UTC over southern Florida. Compare the forecasts with the GOES image of the convective system (Figure 5-13).

Goddard instruments constituted the core of sensors carried on the ER-2 (Figure 5-12), including the MODIS Airborne Simulator (MAS, Platnick/913 and King/900), the Cloud Physics Lidar (CPL, McGill/912), the 95 GHz (3 millimeter) Cloud Radar System (CRS, Heymsfield/912), the 3-cm wavelength (precipitation) ER-2 Doppler radar (EDOP, Heymsfield/912) system and Conical Scanning Sub-mm wave Imaging Radiometer (COSSIR, Wang/975)—a microwave sensor for detection of ice and precipitation. MAS, CPL and CRS provided an effective simulation of key elements of NASA’s planned “A-Train” satellite constellation, especially as regards sensing of upper tropospheric clouds, i.e., Aqua/MODIS, CALIPSO and CloudSat.

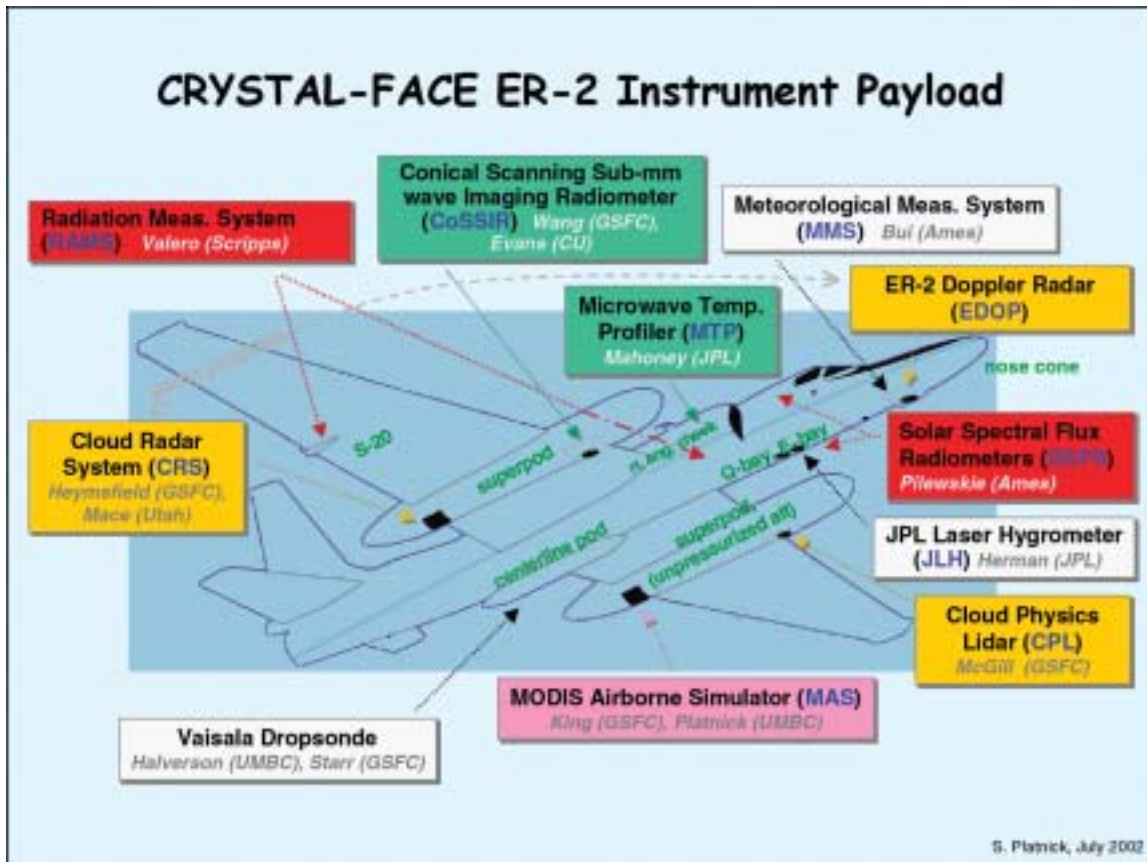


Figure 5-12. Instrument layout on NASA’s ER-2 for CRYSTAL-FACE field deployment in July 2002.

Coincident data from the instruments are shown in Figure 5-13, where the complementary nature of the observations is readily apparent. Cirrus clouds are a particularly difficult remote-sensing target due to their lack of optical opacity and great variability. Combination of multiwavelength observations from active and passive sensors holds the greatest promise of enabling detailed accurate retrievals of cirrus cloud properties. This was the first CRS mission and the first time coincident MAS, CPL and CRS data have been obtained.

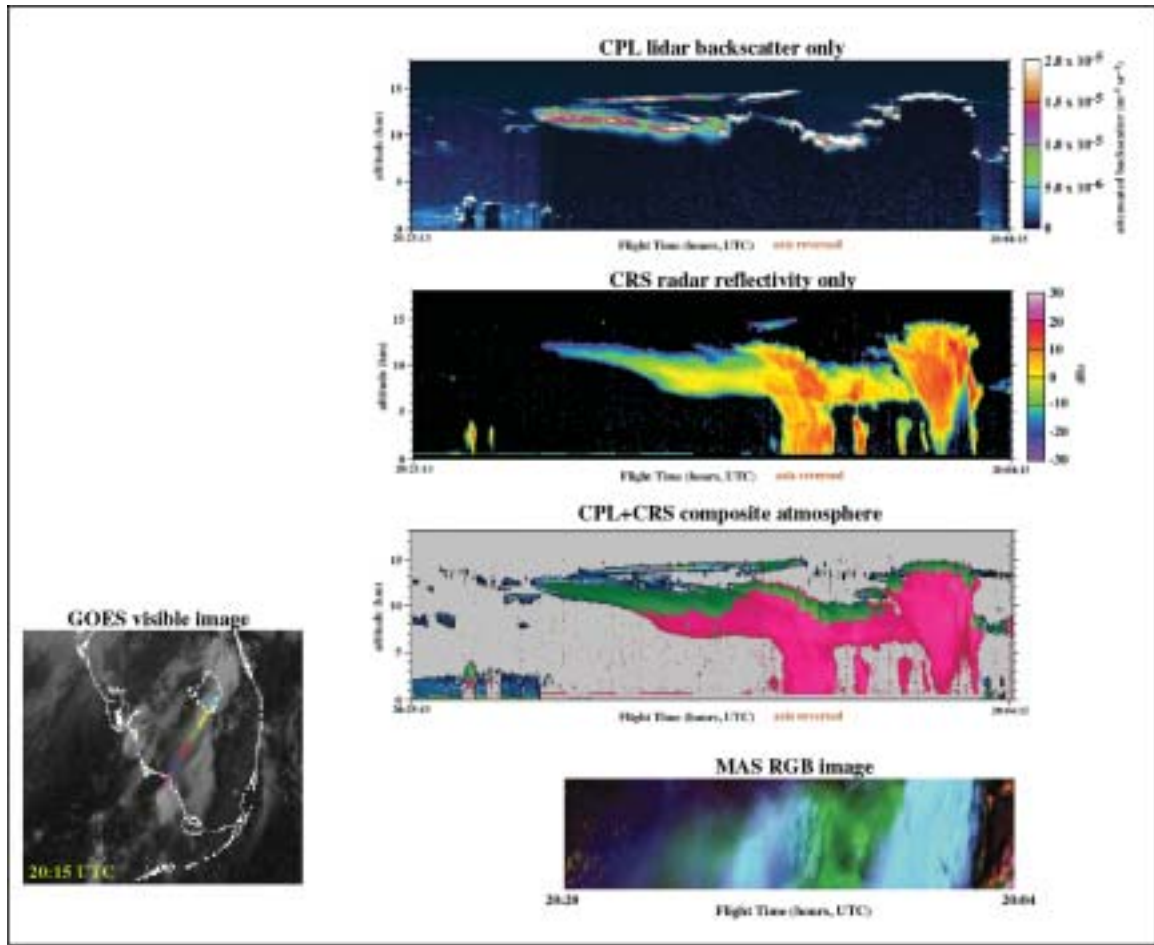


Figure 5-13. GOES image (lower left) shows generating convective system on July 23, 2002, near Lake Okeechobee with cirrus anvil streaming to southwest and overlaid 15-minute aircraft tracks at about this time. Shown are concurrent CPL and CRS profile images of cloud properties along the ER-2 flight track, as well as combined image. The latter depicts the cloud regions detected only by lidar (blue), by both lidar and radar (green), and only by radar (pink). A concurrent MAS image of the scene is shown at the bottom.

Special radiosonde observing support (3-hourly soundings on operational days) by the National Weather Service Forecast Offices at Tampa, Miami, and Key West was arranged and coordinated by Goddard (Starr/912). Special arrangements were also made to acquire a very complete NWS NEXRAD data set for the experiment from these same sites, as well as from the NWS Melbourne site, using a new system to enable real-time data transmission to GSFC (Rickenbach/JCET/912). A new ER-2 dropsonde system (Halverson/JCET/912), developed and operated by NCAR in collaboration with NASA, was used to obtain profiles of atmospheric state when the aircraft was far from operational sites (missions were flown to the deep tropics southeast of the Yucatan Peninsula (Figure 5-14)), and to characterize the offshore preconvective and anvil environments. A mobile radiosonde system (Halverson/JCET/912) was also operated in the interior of southern Florida by staff from the University of Central Florida, and sondes were provided for the western Everglades City remote-sensing site manned by scientists from PNNL (DOE).

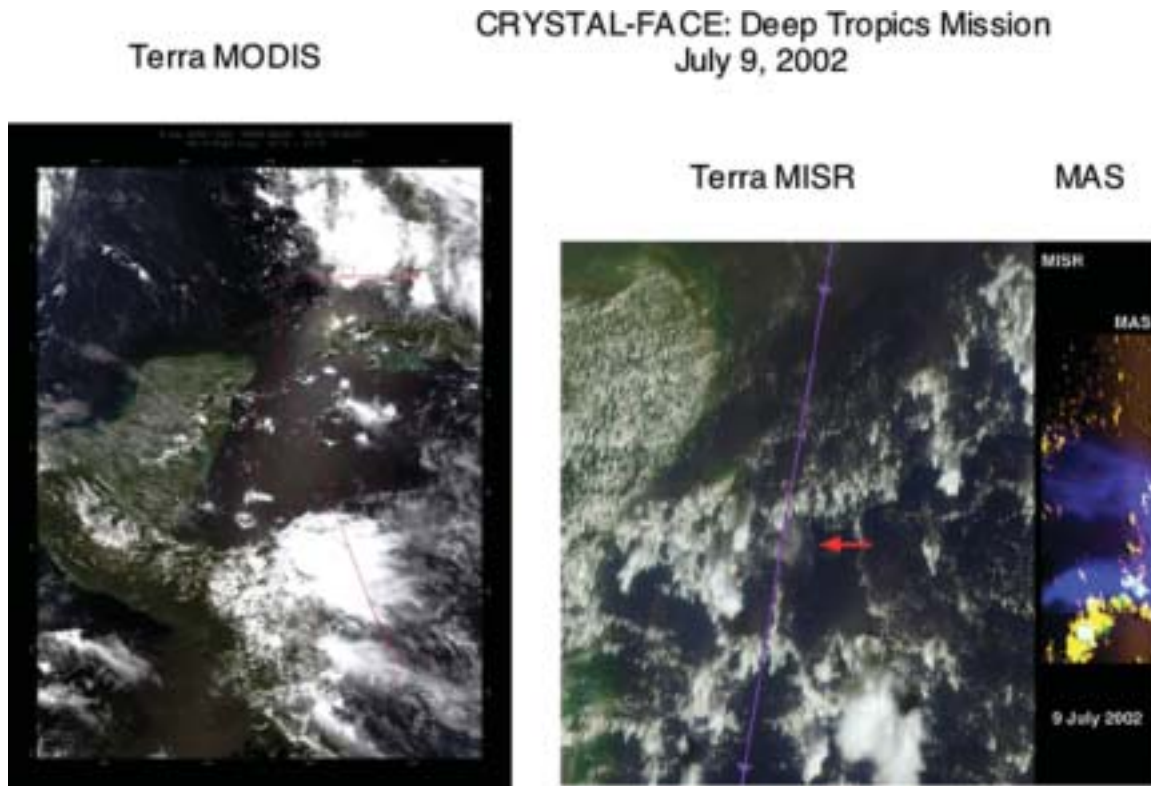


Figure 5-14. MODIS, MISR and MAS imagery during deep tropics mission to study tropical tropopause transition layer. MISR image courtesy of Ralph Kahn/JPL.

Additional information on CRYSTAL-FACE may be found at the following Web sites: <http://cloud1.arc.nasa.gov/crystalface/index.html> and <http://angler.larc.nasa.gov/crystal/>

Climate and Radiation Branch, Code 913

Branch Summary

As we embark upon the new millennium, one of the most pressing issues we face is to understand the Earth's climate system and how it is affected by human activities now and in the future. This has been the driving force behind much of the activities of the climate and radiation branch. We have made major scientific contributions in five key areas: hydrologic processes and climate, aerosol-climate interaction, clouds and radiation, model physics improvement, and technology development. They are highlighted at the end of this section.

Besides scientific achievements, we have made great strides in many areas of science leadership, as well as science enabling, education, and outreach. Thanks to the organization efforts of Yoram Kaufman and Lorraine Remer, the Aerocenter visitor program has been established and is in full operation. The Aerocenter seminar series is running well and is very well attended. We have over 10 visitors already planning to visit and interact with scientists at the Lab during 2002–2003. The processing of MODIS aerosol and cloud products, including the development of cloud masks for aerosols, cloud optical thickness and cloud microphysics are going well. The MODIS aerosol group has produced the first quantitative, accurate, operational aerosol product over most land surfaces. The MODIS aerosol retrieval over oceans reduces the standard error by half when compared to the product accuracy of heritage satellite retrievals (e.g., AVHRR). The availability of MODIS cloud and aerosol products has opened many pathways of research in climate modeling and data assimilation in the Laboratory.

We actively participated and played lead roles in the Cirrus Regional Study of Tropical Anvils and Cirrus Layers-Florida Area Experiment (CRYSTAL-FACE) field campaign held in Key West, Florida, during July 2002. CRYSTAL-FACE studied the life cycle and radiative and microphysical properties of anvil cirrus, and involved 6 aircraft, 2 ground stations, and several hundred scientists. The ER-2 logged over 70 flight hours and flew several new instruments. The combined instrument payload of the ER-2 and Proteus aircraft constituted an “A-train” simulator for the upcoming series of satellites (Aqua, CloudSat, Calypso, Parasol). CRYSTAL-FACE objectives also included relating anvil properties to convective intensity, understanding the exchange of water vapor in the upper troposphere and lower stratosphere, and validation of remote-sensing techniques.

We continued to serve in key leadership positions on international programs, panels and committees. Si-Chee Tsay leads a group of scientists from NASA and universities in initiating a new project, BASE-ASIA, to study impacts of smoke aerosols on tropospheric chemistry, water and carbon cycles, and their interactions in the Southeast Asia monsoon region, using multiplatform observations from satellites, aircraft, networks of ground-based instruments and dedicated field experiments. Robert Cahalan has served as project scientist of SORCE (Solar Radiation and Climate Experiment), which was launched in December 2002, and will measure both TSI (Total Solar Irradiance, formerly “solar constant”) and SSI (Spectral Solar Irradiance) with unprecedented accuracy and spectral coverage (1–2000 nm for SSI, 1–100,000 nm for TSI) during a 5-year nominal mission lifetime. During the past year, Warren Wiscombe has been appointed as Science Lead for the Earth Science Vision 2025 activity commissioned by NASA Headquarters. This involves forming science workgroups drawn from NASA Centers and the community at large to decide on specific science questions for NASA's far future in Earth science.

The Earth Observatory Web site (<http://earthobservatory.nasa.gov>) has continued to provide the science community with direct communication gateways to the latest breaking news on NASA Earth sciences. It provides the news media and other communications outlets with a “one-stop shopping” resource for publication quality images and data visualizations from NASA Earth science satellite missions such as Terra, Aqua, and many others. The Earth Observatory Web site now boasts over 27,000 subscribers, with roughly 1 million page views per month worldwide. The contents of the Web site are increasingly syndicated by NASA Headquarters and other public sites.

Science Highlights

Atmospheric Hydrologic Processes and Climate

Summertime climate teleconnection

Using NCAR/NCEP reanalysis and GPCP rainfall data, we have identified recurrent climate modes associated with sea surface temperature (SST) variability in the North Pacific and the North Atlantic that are distinct from El Niño. Simultaneous high/dry (or cool/wet) summers were found over Japan/Southern Korea, northwestern North America, and the northern Great Plains, and reverse conditions over the Atlantic coasts. These modes may be instrumental in simultaneously altering the probability distribution of extreme temperature and rainfall events in Eurasia and North America, and providing potential predictability of flood and drought occurrence over the two continents.

Canonical Ensemble Predictions

We have developed a canonical ensemble prediction (CEC) scheme for the seasonal rainfall over the U.S. continent to maximize the predictive information from a variety of sources, e.g., SST from various ocean basins and soil moisture. In benchmark hindcast experiments, CEC shows an overall increase in potential predictability of 15–20% over traditional methods, with most gain in the summer season, when the El Niño influence is weakest. The CEC methodology is being adopted at NCEP for seasonal forecasts. CEC can also be incorporated into multimodel statistical-dynamical forecasts to achieve overall better forecast skills.

Rainfall retrieval

Simultaneous observations of reflectivity made by TRMM Precipitation Radar (PR) and brightness temperature, T_b , made by Microwave Imager (TMI) radiometer over tropical land are being analyzed with the help of theoretical models to understand the relationship between these two data sets. TRMM PR data analyses over land reveal that there is a significant variability in the strength of convection over different geographical regions. We are investigating this regional variability in convection and its impact on rain retrievals with the TRMM TMI data. Preliminary results from our study indicate that it is possible to deduce a parameter from T_b that can account for regional variability in convection. This study can enhance the capability of satellite-borne microwave remote sensors.

Rainfall sampling

A statistical model for the variability of rain in time and space has been applied to gain better understanding of the level of disagreement to be expected between satellite observations over areas containing rain gauges and the average rainfall measured by the gauges themselves. The model suggests how best to choose the area around the gauges over which the satellite observations are averaged and the time intervals over which the gauge data are averaged in order to minimize the magnitude of the difference between the two averages. The results are very helpful in evaluating the accuracy of satellite rain estimates with surface gauges.

Regional effects of global warming

Using the NCAR regional climate model, we are studying the elevation dependence of the surface temperature warming over the Tibetan Plateau (TP) due to doubling CO_2 . In the eastern TP, when CO_2 is doubled, the cloud amount increases at lower elevations and decreases at higher elevations in the winter half year. As a consequence, at lower elevations the short wave solar radiation absorbed at the surface declines and the downward long wave flux reaching the surface enhances; on the other hand, at higher elevations the surface solar radiative flux increases and the surface infrared flux shows a more uniform increase. The net effect of the changes in both radiative fluxes is an enhanced surface warming at higher elevations, which is the primary cause of the elevation dependency in the surface warming. In the southwestern TP, the most significant factor affecting the surface energy budget is the depletion of snow cover at higher elevations, which leads to a reduction of the surface albedo, and increase in surface temperature.

Climate variability of South America

The submonthly variability of atmospheric circulation and organization of convection in South America during JFM98 and JFM99 was studied (January-February-March). According to the NCEP reanalysis, the South America Low Level Jet (SALLJ) was nearly twice as strong during JFM of the 1998 El Niño episode than during JFM of the 1999 La Niña episode. The difference in SALLJ strength between these two years translated into stronger transport of moist tropical air into the subtropics during JFM98 than during JFM99. An objective analysis technique was used to identify large, long-lived convective cloud systems in infrared imagery. The stronger SALLJ resulted in larger and more numerous long-lived convective cloud systems and nearly twice as much rainfall in subtropical South America during JFM98 than during JFM99. While the SO (Southern Oscillation) modulates the SALLJ in interannual timescales, the SACZ (South Atlantic Convergence Zone) modulates the SALLJ in submonthly timescales. Both time scales are found in rainfall variability in the South America subtropical region.

Regulation of warm pool SST

The sea surface temperature (SST) of the tropical western Pacific (Pacific warm pool) is very high but rarely greater than 30°C. It is very important to understand the physical processes that prevent the temperature from increasing to a value higher than 30½, as it will shed light on the possible scenarios of global warming of the tropical oceans. By analyzing the surface wind, clouds, and the surface heat fluxes in the warm pool, we have found that regions of the highest SST have the largest surface heating, primarily due to the weak evaporative cooling associated with weak winds. Results show that an enhanced surface heating in an enhanced convection region is not sustainable and must be interrupted by variations in large-scale atmospheric circulation.

Aerosol-Climate Interactions

Distinguishing man-made vs. natural sources of aerosol

Plumes of smoke and regional pollution are distinguished by their large concentrations of small particles (less than 1 micrometer) downwind of biomass burning sites and urban areas. New analysis of 2 years of daily global data collected by the Moderate Resolution Imaging Spectroradiometer (MODIS) instrument flying aboard NASA's Terra and Aqua satellites is allowing us to distinguish small from large aerosol particles by measuring precisely the aerosols' reflection of sunlight across most of the solar spectrum (from 0.41 to 2.2 micrometers). These measurements of pollution and smoke airborne particles are important because, depending upon the type of particles produced, human pollution can either have a warming or cooling influence on climate, and they can either increase or decrease regional rainfall. The results were reported in the September issue of Nature in a review paper on the satellite view of aerosol effect on climate

Validation of MODIS aerosol optical thickness

A preliminary evaluation of the MODIS aerosol products had been completed in 2000, using a limited data set of just 2–3 months of data, consisting of less than 400 points. Those results suggested that MODIS was retrieving aerosol optical thickness to within the prelaunch expected accuracy. MODIS has now been collecting data and producing an aerosol product for over 2 years. Recently, we completed a more thorough evaluation. The MODIS satellite-derived products are co-located with ground-based AERONET sunphotometers, and the aerosol optical thickness produced by each type of instrument are compared. AERONET is expected to be accurate to within 0.01 of optical thickness units, and is taken to be the ground "truth." Over two full years of data consisting of 2052 ocean points from 44 coastal and island AERONET stations and 5908 land points from 96 land AERONET stations have been compared.

Clouds and Radiation

Atmospheric radiative transfer

A simple approach has been developed that uses theoretical simulations to estimate the uncertainties that arise in cloud optical thickness retrievals due to neglect of cloud horizontal variability. For the first time, preliminary error bounds have been set to estimate the resulting errors for stratocumulus clouds. Another approach was proposed that combines visible and thermal infrared images to see whether 3-D radiative effects make clouds appear asymmetric. These results help us understand the uncertainties that horizontal cloud variability introduces into retrievals of cloud optical thickness, an important product of MODIS.

Shortwave radiation in cloudy atmosphere

Using an improved geometric-optics method, Yang et al. [2000] had computed the single-scattering optical properties of individual ice particles as a function of particle habit (shape), particle size, and wavelength. Based on these precomputed single-scattering optical properties, we have computed the mean effective particle size, mass absorption coefficient, single-scattering albedo, and asymmetry factor for 30 sample cirrus clouds in both the tropics and middle latitudes. Each sample cloud is identified with a particle size distribution, a composition of particle habits, and the aspect ratios of particle size dimension. We then developed parameterizations for the bulk mass absorption coefficient, single-scattering albedo, and asymmetry factor as a function of the mean effective particle size. The new fast and accurate parameterization has been implemented into the Goddard radiation scheme for use in cloud and climate models.

International intercomparison of 3-dimensional Radiation Codes (I3RC)

I3RC is an ongoing joint activity of NASA and DOE that encourages development and testing of multiangle atmospheric radiative transfer codes. This activity involves 32 research groups in 6 countries, who met for workshops in 1999 and 2000, and are now developing an “open source” 3-D Monte Carlo code for general distribution. An executive committee of I3RC participants, chaired by Robert Cahalan of the Branch, and other 3-D modelers, are now organizing a 3-DRT (3-dimensional Radiative Transfer) Working Group, under the auspices of the IRC (International Radiation Commission).

Physical Parameterizations

Cumulus and stratiform cloud parameterization

Three major upgrades to the cumulus parameterization scheme in the new NASA/NCAR climate model have been implemented. First, the cloud-base mass flux in moist convection was assumed to ensue with saturated as opposed to grid-averaged specific humidity. Second, the conditionally unstable clouds were forced to rise, depleting some of the excess specific humidity as cloud water and precipitation. Third, Relaxed Arakawa-Schubert Scheme (RAS) was reconfigured to simulate atmospheric boundary layer (BL) eddies to transport heat and moisture up into the inversion layer. The results show that these upgrades represent a significant step in the right direction. The GCM simulated some of the key features of the Indian drought of 1987 and North American drought of 1988 with some useful skill.

Shallow convection scheme in AGCM

Major modifications were undertaken in the physical parameterizations used by the NSIPP atmospheric general circulation model. These modifications were aimed primarily at improving the model’s simulation of boundary layer clouds over ocean, especially maritime stratus decks and the stratus-trade cumulus transition. A prognostic cloud condensate scheme was implemented, as well as a shallow convection/PBL entrainment parameterization scheme. Along with the introduction of these new physical processes, changes to pre-existing parameterization schemes, including convection, radiation and turbulence schemes were also made. Recent results with the NSIPP AGCM suggest that vigorous transport of water vapor between 800mb to 500mb may be the key to eliminating the spurious, southern ITCZ.

Technology Development

THOR (THickness from Offbeam Returns)

THOR had its initial validation flights on the NASA P3B, over the Oklahoma ARM site in March 2002, demonstrating THOR's ability to measure physical thickness of dense cloud layers. THOR's capabilities are now being extended to measure thickness of sea ice layers, with the addition of several angular channels. THOR is expected to fly over Antarctic sea ice in August 2003. THOR development is being led by Robert Cahalan (913), with co-investigator Matthew McGill (912) and chief engineer John Kolasinski (565).

Aerosol detection instrumentations

We have also designed and built two new instruments in the aerosol group: 1) Aerosol Multiple Reflection Extinction Cell, in response to the lack of standard in situ measurements of aerosol absorption, and 2) the Cloud Scanner Spectrometer, aimed at studying the interaction between aerosols and clouds. The first prototype of the multiple reflection extinction cell has been built and is being tested and calibrated, and the Cloud Scanner Spectrometer was tested for the first time during the SMOCC/LBA experiment in Brazil, in October 2002.

SMART (Surface Measurement of Atmospheric Radiative Transfer)-COMMIT (Chemical, Optical and Microphysical Measurements of in situ Troposphere)

The GSFC SMART consists of a suite of remote-sensing instruments, including many commercially available radiometers, spectrometer, interferometer, and three in-house developed instruments: micro-pulse lidar (MPL), scanning microwave radiometer (SMiR), and sun-sky-surface photometer (S3). During past years, SMART has been deployed in many NASA-supported field campaigns to collocate with satellite nadir overpass for intercomparisons, and for initializing model simulations. Built on the successful experience of SMART, we are currently developing a new ground-based in situ sampling package, COMMIT, including measurements of trace gases (CO, SO₂, and O₃) concentrations, fine/coarse particle sizers and chemical composition, single- and three-wavelength nephelometers, and surface meteorological probes. The next major activities for SMART-COMMIT are scheduled for FY03-05 in BASE-ASIA (Biomass-burning Aerosols in South East-Asia) and CHINA-TEA (Climate & Health Impacts in Northeast Asia-Tropospheric Experiment on Aerosols)

Unified Onboard Processing and Spectrometry (UniOPS)

A group of scientists and engineers at GSFC, led by Si-Chee Tsay, is funded by ESTO/ACT in a new project to unify onboard processing techniques with compact, low-power, low-cost, Earth-viewing spectrometers being developed for eventual space missions. The philosophy is that spectrometry and its onboard processing algorithms must advance in lockstep, and eventually unite in an indistinguishable fashion. A future is envisioned in which archives of the spectrometer outputs will not be a monstrous data-dump of spectra, but rather an entity that contains the full information content of the spectra, compressed on board into much smaller and more valuable data streams. Preliminary results show that compression factors of 10 to 100 are possible using a combination of physics-based removal and proximal differencing.

In the next few short articles we highlight some of the science achievements of the Branch.

Shallow Convection Scheme in AGCM

By Julio Bacmeister (bacmj@janus.gsfc.nasa.gov)

Low-level stratus and stratocumulus (St/Sc) cloud decks are a persistent feature over the relatively cool waters of eastern subtropical oceans. Well-known examples are the “fog banks” off the coasts of California and Peru. These cloud decks can be extensive, covering areas the size of the continental U.S. They reflect incoming sunlight much more effectively than the ocean underneath, and for this reason reduce the amount of solar radiation that is absorbed by the Earth. The combination of their persistence, large size, and strong radiative effect means that marine St/Sc decks are a critical component of the Earth’s net radiation budget. Modest changes in stratus deck extent could enhance (or mitigate) changes in climate induced by greenhouse gases.

Unfortunately, correctly simulating the cloud-topped marine boundary layer (MBL) in atmospheric general circulation models (AGCMs) remains a vexing problem. To begin with, stratus decks though very extensive in the horizontal, are thin, often no more than 100 to 200 meters thick. This represents a severe challenge to AGCMs whose vertical grid spacing is normally larger than this. Even with sufficient vertical resolution the creation and destruction of marine St/Sc decks involves processes that are poorly represented in AGCMs: moist turbulence and shallow convection, cloud/radiation interaction, and cloud microphysics. Numerous scientists have suggested that the key to simulating realistic St/Sc decks lies in correctly diagnosing the rate of entrainment at the top of the MBL (e.g., Grenier and Bretherton 2001). Moisture and potential temperature gradients at the top of the stratus-capped MBL are strong, so that small differences in turbulent transport can have a large impact on cloud distributions. Standard dry turbulence schemes tend to underestimate PBL-top entrainment, leading to overly wet, cool marine BLs and excessive low cloud cover. Proposed explanations for insufficient entrainment are that physical processes such as radiative destabilization in cloud decks (e.g., Stevens et al. 1999), evaporatively driven downdrafts (e.g., Deardorff 1980), and overshooting moist thermals (e.g., Stull 1989) are not included in most dry turbulence schemes.

The NSIPP AGCM includes a simple 1st-order, dry PBL scheme (Louis et al. 1983). The scheme appears to perform well in many respects, such as in its overall reproduction of tropical temperature and moisture profiles. However, without modification, the scheme leads to excessive low-level cloudiness throughout the subtropics. In order to overcome this problem, a relatively simple, plume-based entrainment calculation was added to the basic Louis scheme. This calculation is accomplished using a 1-D linearly entraining moist plume model to estimate the strength of overshooting moist thermals originating from the surface layer. The vertical momentum equation used for the plume includes condensational buoyancy production as well as liquid water loading. The vertical velocity w_u within the plumes is used to calculate an additional diffusivity,

$$K_{zz,u}(z) = a_u w_u(z) \delta_{BL},$$

which is applied near the MBL top. The parameter, a_u , is a constant representing roughly the areal fraction of a gridbox covered by moist updrafts, δ_{BL} is a length scale determined from the depth of the boundary layer. For definiteness we take δ_{BL} to be 20% of the boundary layer depth, defined as the level where the entraining plume becomes neutrally buoyant, and regard a_u as a tunable constant.

Figure 5-15a shows low-level (below 700 mb) cloud fraction for June 1989 from a simulation using a “reasonable” value of $a_u=0.03$, that is 3% of a typical gridbox covered by moist updrafts. The basic structure of the cloud fields compares reasonably well with ISCCP observations (Fig. 5-15b), with dense, low-level cloud decks found off the coasts of California, Peru, and Namibia as well sparser cloud decks off of Australia and near the Azores. Cross sections of cloud fraction (Fig. 5-15c) and cloud condensate (Fig. 5-15d) are shown along 26N (California stratus). The simulation in Fig. 5-15 appears to underestimate cloudiness, except in the arctic. The cloud cross sections in Figs. 5-15c and 5-15d, exhibit cloud decks that have a generally realistic appearance. The decks are

too low, reaching only 900 mb before dissipating, whereas in reality Sc cloud top heights reach 800 mb or higher before dissipating. The highest cloud fractions in the simulated California St/Sc deck are found near the coast, but are found somewhat further out over ocean in reality. The primary mechanism for cloud production in the simulated California stratus deck is found to be large-scale condensation. However, west of 150W and above 900 mb, the primary source of condensate is from detraining convection. This is encouraging because it may be analogous to the stratocumulus to trade cumulus transition in nature, which occurs as shallow convection rather than moist turbulence becomes the source of condensate (e.g., Wyant et al. 1996). The secondary cloud deck in the simulation is sparse with fractions only between 10% and 30%, but reaches heights more consistent with observed Sc and trade cumulus tops.

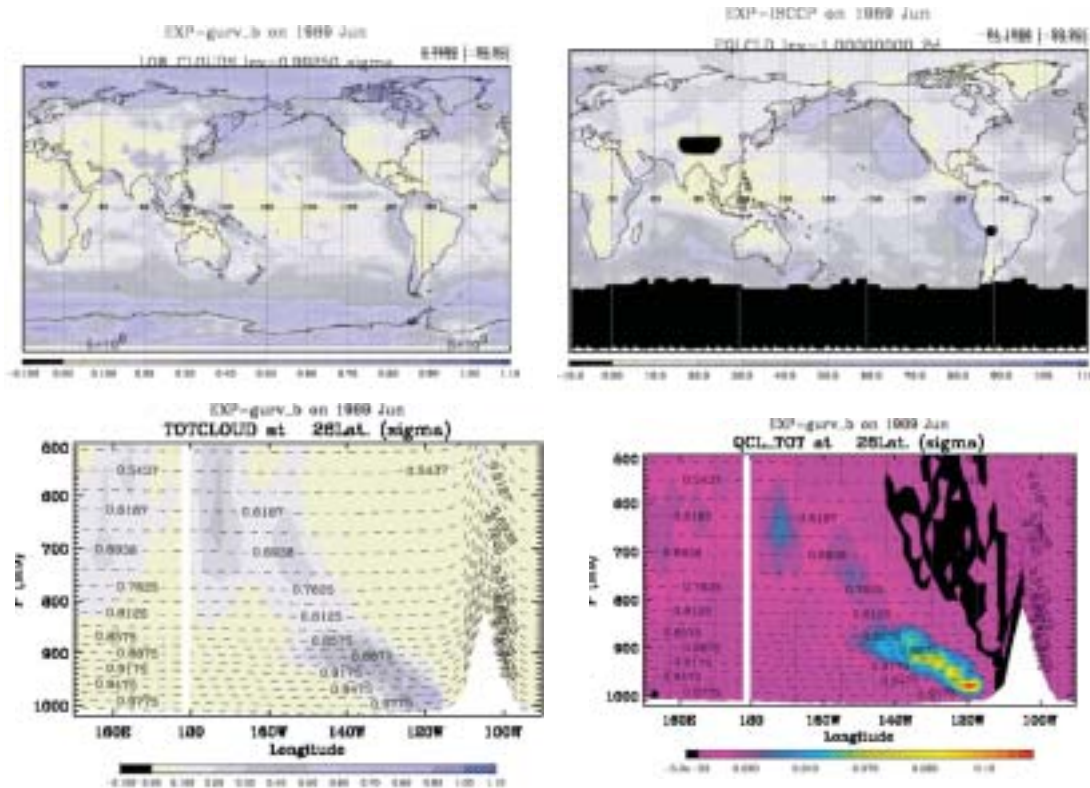
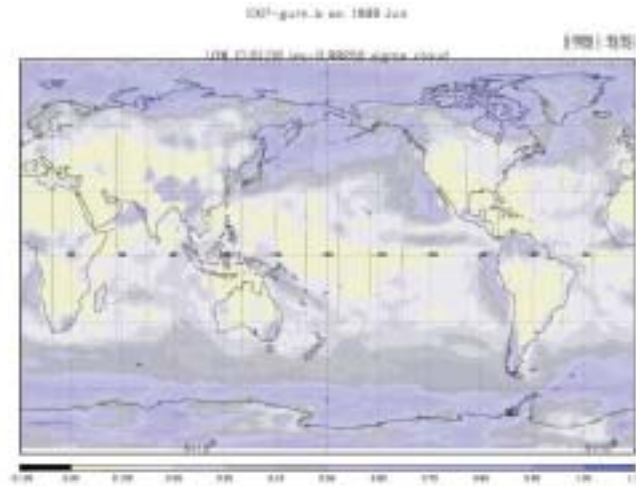
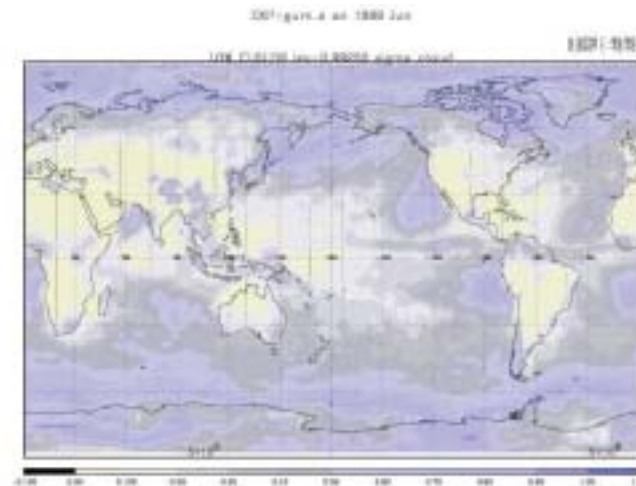


Figure 5-15. (a, upper left) low level (>700mb) cloud cover for June 1989 from the NSIPP AGCM with prognostic clouds and PBL entrainment; (b, upper right) ISCCP low cloud fraction for June 1989; (c, lower left) longitude-pressure section along 26N-California stratus region-of cloud fraction from the model; and (d, lower right) longitude-pressure section along 26N of cloud condensate mixing ratio (g/kg).

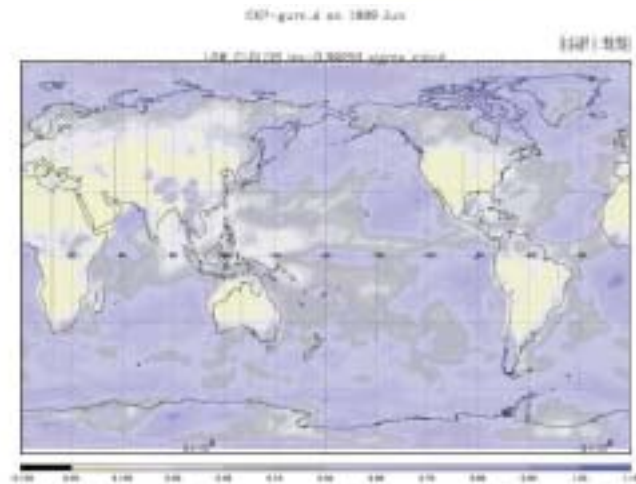
Figure 5-16 shows the sensitivity of the simulated low-level cloudiness to the assumed updraft areal fraction a_u . Figure 5-16a repeats results for $a_u=0.03$. Figures 5-16b and 5-16c show that, as expected, the effect of reducing a_u is to increase the amount of low-level cloudiness. In Figure 5-16c with $a_u=1 \times 10^{-5}$ dense low-level clouds occur almost everywhere above the boundary layer. With $a_u=1 \times 10^{-2}$ (Figure 5-16b) low-level cloudiness distributions are in good agreement with observations. However, cross sections of the cloud fields in Figure 5-16b reveal similar defects to those shown in Figures 5-15c, d, i.e., cloud tops near 900 mb, and weak production of clouds by convective detraining. It should be emphasized that the “best” choice for a_u will probably depend on other choices made in the model physics parameterizations. The basic point of Figure 5-16 is simply to illustrate the control of a_u on low-level cloudiness for a given set of model parameters.



5-16a



5-16b



5-16c

Figure 5-16. Sensitivity of low-level cloudiness to entrainment parameter a_u ; a) strong entrainment $a_u=3 \times 10^{-2}$, b) moderate entrainment $a_u=1 \times 10^{-2}$, and c) weak entrainment $a_u=1 \times 10^{-5}$. Cloud fields for June 1989 are shown.

The results shown above are encouraging in that they show that reasonable cloud simulations may be obtained in a model using a relatively simple extension to a 1st-order PBL scheme. However, the results are somewhat unsatisfying in that they require a separate ad hoc moist plume model. Similar results should be possible by modifying the model's existing convection scheme –RAS (Moorthi and Suarez 1992) to better simulate shallow convection. Such an effort is now underway, and appears promising.

Deardorff, J.W., 1980: Cloud-top entrainment instability. *J. Atmos. Sci.*, **37**, 131-147.

Grenier, H. and C.S. Bretherton, 2001: A moist PBL parameterization for large-scale models and its application to subtropical cloud-topped marine boundary layers. *Mon. Wea. Rev.*, **129**, 357-377.

Louis, J., M. Tiedtke, J. Geleyn, 1982: A short history of the PBL parameterization at ECMWF, in *Proceedings, ECMWF Workshop on Planetary Boundary Layer Parameterization, Reading, U.K.*, 59-80

Moorthi, S., and M.J. Suarez, 1992: Relaxed Arakawa-Schubert: A parameterization of moist convection for general circulation models, *Mon. Weather Rev.*, **120**, 978-1002.

Stevens, B, C.-H. Moeng, and P.P. Sullivan, 1999: Large-eddy simulations of radiatively driven convection: Sensitivities to the representation of small scales. *J. Atmos. Sci.*, **56**, 3963-3984.

Stull, R., 1989: *An Introduction to Boundary Layer Meteorology*, Dordrecht-Kluwer, 666 pp.

Wyant, M.C., C.S. Bretherton, H.A. Rand, D.E. Stevens, 1996: Numerical Simulations and a conceptual model of the stratocumulus to trade cumulus transition, *J. Atmos. Sci.*, **54**, 168-192.

A New Satellite View of Aerosols in the Climate System

By Yoram J. Kaufman (Yoram.J.Kaufman@nasa.gov)

Manmade aerosols reflect sunlight to space, cooling the Earth's surface; at the same time they absorb solar radiation thereby warming the atmosphere. Aerosols affect cloud properties and precipitation patterns. High concentrations of aerosols with varying compositions are found downwind of urban and industrial areas, regions of domestic and forest fires, and deserts. Study of this global heterogeneous aerosol requires continuous observations from satellites, networks of ground-based instruments, and dedicated field experiments. These measurements show that aerosols have large radiative impacts downwind of polluted continental regions and deserts. Future trends in aerosol composition and concentration driven by industrialization and population expansion may adversely affect the Earth's climate, water supply, and human health.

During the last century, the Earth's surface temperature increased by 0.6°C, reaching the highest levels in the last millennium. This rapid temperature change is attributed to a shift of less than 1% in the energy balance between absorption of incoming solar radiation and emission of thermal radiation from the Earth system. Among the different agents of climate change, anthropogenic greenhouse gases and aerosols play the larger roles. While greenhouse gases reduce the emission of thermal radiation to space, thereby warming the surface, aerosols mainly reflect and absorb solar radiation (the aerosol direct effect) and modify cloud properties (the aerosol indirect effect), cooling the surface. These impacts on the radiation balance are very different and therefore require different research approaches.

Greenhouse gases, such as carbon dioxide and methane, have a long lifetime in the atmosphere of 100 years and a rather homogeneous distribution around the globe, in contrast to the heterogeneous spatial and temporal distribution of tropospheric aerosols due to their short lifetime of about a week. As a result, the global increase in the carbon dioxide concentration of 1–2 ppm per year was measured half a century ago using a single ground-based instrument, while daily satellite observations and continuous ground-based measurements are needed to observe the emission and transport of dense aerosol plumes downwind of populated and polluted regions (urban haze), regions with vegetation fires (smoke), and deserts (dust). The effect of greenhouse gases on the energy budget occurs everywhere around the globe. Aerosols have both regional and global impacts on the energy budget, requiring frequent global measurements tied to elaborate aerosol models that realistically represent the atmospheric aerosols.

Aerosol effects on climate differ from those of greenhouse gases in two additional critical ways. Because most aerosols are highly reflective, they raise our planet's albedo, thereby cooling the surface and effectively offsetting greenhouse gas warming by anywhere from 25% to 50%. However, aerosols containing black graphitic and tarry carbon particles (present in smoke and urban haze), are dark and therefore strongly absorb incoming sunlight. The effects of this type of aerosol are twofold, both warming the atmosphere and cooling the surface before a redistribution of the energy occurs in the column. During periods of heavy aerosol concentrations over the Indian Ocean and Amazon Basin, for example, measurements revealed that the black carbon aerosol warmed the lowest 2–4 km of the atmosphere while reducing by 15% the amount of sunlight reaching the surface. Heating the atmosphere and cooling the surface below reduces the atmosphere's vertical temperature gradient and therefore is modeled to cause a decline in evaporation and cloud formation over the Mediterranean region. On the other hand, global circulation models show that the aerosol warming can change the regional and global circulation, bringing moisture and floods to Southern China due to the presence of the nearby Pacific Ocean.

The second way in which aerosols differ from greenhouse gases is through the aerosol effect on clouds and precipitation. In polluted regions, the numerous aerosol particles share the condensed water during cloud formation, therefore reducing cloud droplet size by 20%–30%, causing an increase in cloud reflectance of sunlight by up to 25%, and cooling the Earth's surface. The smaller, polluted cloud droplets are inefficient in producing precipitation, so they may ultimately modify precipitation patterns in populated regions that are adapted to present precipitation rates. The cooling effect due to polluted clouds is still poorly characterized with an uncertainty 5 to 10 times larger than the uncertainty in the predicted warming effect of greenhouse gases. The effect of aerosols on precipitation is even less well understood.

To assess the aerosol effect on climate we first need to distinguish natural from anthropogenic aerosols. Satellite data and aerosol transport models show that plumes of smoke and regional pollution have distinguishably large concentrations of fine (submicron) size aerosols (see Figures 5-17,5-18,5-19). In contrast, natural aerosol layers may have concentrated coarse dust particles and only widespread fine aerosols from oceanic and continental sources. The new ability of satellites to observe the spatial distribution of aerosol and to distinguish fine from coarse particles (Figure 5-17) can be exploited to separate natural from anthropogenic aerosols. In situ measurements of aerosol composition and size, models that assimilate the measurements and information on population density and economic activities are needed to further quantify the anthropogenic aerosol component, and to relate it to specific aerosol sources.

Aerosol research is in transition from an exploratory phase to a global quantitative phase. In the exploratory phase, new aerosol related processes are discovered, i.e., the large concentration of black carbon emitted from vegetation fires and found in regional pollution in the tropics and its effect on slowing down the hydrological cycle; the effect of aerosol on reducing precipitation efficiency and counteracting regionally the greenhouse warming. In this phase models are used to assess the potential of aerosol processes to affect the global climate. Because aerosols vary widely from region to region, a multiple-measurement approach is necessary to assess their impacts on global climate. Specifically, we require the use of long-term, detailed global measurements from satellites, distributed networks of ground-based instruments, and comprehensive regional experiments in clean and polluted environments, that feed global aerosol and climate models.

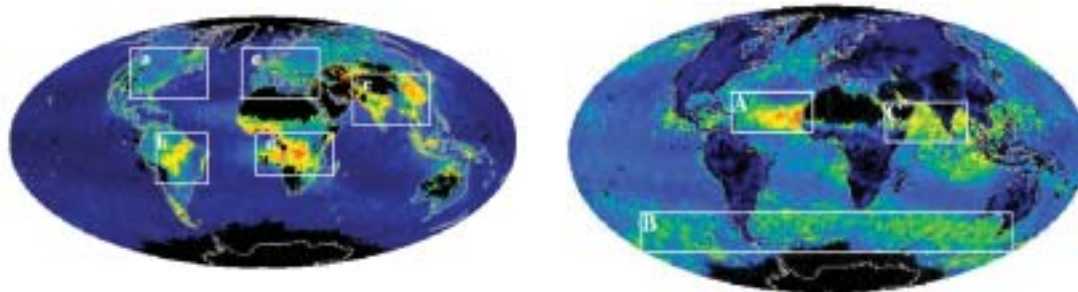
Smoke from fires in Australia—Dec. 25, 2001



Dust emitted from West Africa—Jan. 7, 2002



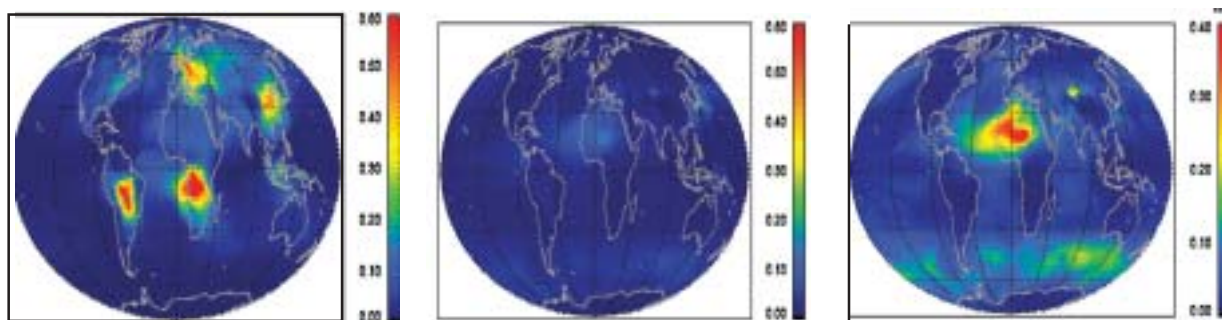
Figure 5-17. Spectral aerosol reflectance measured by MODIS: On the left, color composite of channels in the visible spectrum and on the right for near IR spectrum. Top: Fine smoke particles from fires in Australia (Dec. 25, 2001) invisible over the ocean in the near IR. Bottom: Coarse dust particles emitted from West Africa (Jan. 7, 2002) visible in both panels over the ocean. While dust is clearly visible in the visible and near IR part of the spectrum, the fine smoke particles are mostly transparent in the near IR.



a) Measured fine aerosol optical thickness

b) Measured coarse aerosol optical thickness

Figure 5-18. Global analysis of the fine (left) and coarse (right) aerosol optical thickness ($0.55 \mu\text{m}$) measured from the MODIS instrument on the NASA Terra spacecraft, for September 2000. The optical thickness presented by the color scale, is a measure of the aerosol column concentration. Black regions have surface properties inappropriate for MODIS aerosol retrievals or very low solar elevations. The white boxes indicate regions with high aerosol concentrations. The image shows fine particles in (a) and (c) pollution from North America and Europe, (b) vegetation fires in South America and (d) Southern Africa and (e) pollution in South and East Asia. Coarse dust from Africa (A), salt particles in the windy Southern Hemisphere (B) and desert dust (C).



Man-made fine aerosol optical thickness

Natural fine aerosol optical thickness

Coarse aerosol optical thickness

Figure 5-19. Model results of Chin et al., 2001 that correspond to the MODIS data of September 2000: (a) anthropogenic fine aerosols, (b) natural fine aerosols, and (c) coarse aerosols composed of natural dust and salt. The relationship between the spatial structure between fine anthropogenic aerosol in the model and MODIS is used as indication of the presence of the anthropogenic aerosol.

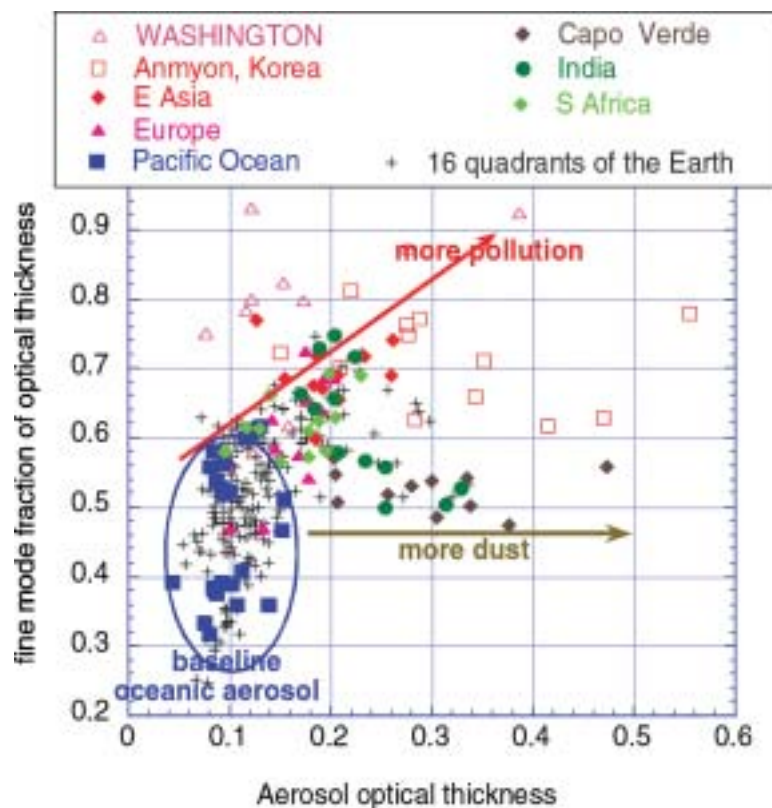


Figure 5-20. Classification of aerosol measured from MODIS over the ocean in 2 dimensions: fraction of the optical thickness due to the fine aerosol versus aerosol optical thickness. The color symbols are for specific locations as indicated and the crosses are for 16 quadrants of the Earth. Each location is represented by one point per month. The baseline aerosol is associated with optical thickness of 0.05–0.10 and fraction of the fine aerosol less than 50%. Dust is associated with higher optical thicknesses and equal fraction of fine and coarse aerosol, while pollution aerosol is associated both with high optical thickness and fine fraction. Note that the data from India are split into the winter pollution group and into the summer dust group.

Kaufmann, Y.J., D. Tanre, O. Bourcher, 2002: A satellite view of aerosols in the climate system. *Nature*, **419**, 215-223.

A New Look into the Effect of Large Droplets on Radiative Transfer Process
By Alexander Marshak (Alexander.Marshak-1@nasa.gov)

Recent studies indicate that a cloudy atmosphere absorbs more solar radiation than any current 1-D or 3-D radiation model can predict. The excess absorption is not large, perhaps 5–15 W/m² or less, but any such systematic bias is of concern since radiative transfer models are assumed to be sufficiently accurate for remote-sensing applications and climate modeling. The most natural explanation would be that models do not capture real 3-D cloud structure and, as a consequence, their photon path lengths are too short. However, extensive calculations, using increasingly realistic three-dimensional cloud structures, have failed to produce photon paths long enough to explain the excess absorption. Other possible explanations have also been unsuccessful, thus at this point, conventional models seem to offer no solution to this puzzle.

The weakest link in conventional models is the way a size distribution of cloud particles is mathematically handled. Basically, real particles are replaced with a single average particle. This “ensemble assumption” assumes that all particle sizes are well represented in any given elementary volume. But the concentration of larger particles can be so low that this assumption is significantly violated. We show how a different mathematical route, using the concept of a cumulative distribution, avoids the ensemble assumption. The cumulative distribution has jumps, or steps, corresponding to the rarer sizes. These jumps result in an additional term, a kind of Green’s function, in the solution of the radiative transfer equation.

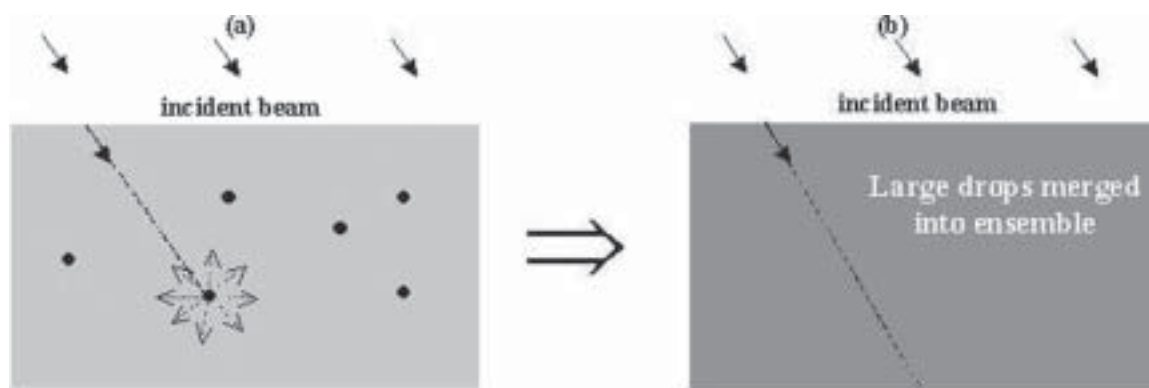


Figure 5-21. (a) Schematic representation of a small cloud piece containing an enormous number of small particles (gray area) and a tiny number of large ones (black dots); and (b) ensemble approach, where the large particles are artificially fractionated and homogenized over space. The true solution to the radiative transfer equation for (a) includes photon interactions with those particles actually present in the cloud, while the ensemble-based approximation (b) accounts for photon interactions with fictitious rare particles included in extremely small concentrations in every elementary volume. The difference between the true solution and the ensemble-based approximation is the Green’s function, which describes the radiation field generated by photons scattered from rare, large particles.

This true solution also exhibits a jump-like behavior, involving two different mathematical mechanisms in the accumulation of energy absorbed by particles. The first one integrates absorption over the photon path, so that the longer the photon path, the larger the amount of energy absorbed by particles. The second mechanism, missed in the ensemble approach, adds up jumps in the true solution corresponding to the rarer particle sizes, each corresponding to a negligible photon path. Solving the cloud radiative transfer equation with the measured particle distributions, described in a cumulative rather than an ensemble fashion, may lead to increased cloud absorption of the magnitude observed.

These results are reported in the paper, “A Missing Solution to the Transport Equation and its Effect on Estimation of Cloud Absorptive Properties,” by Y. Knyazikhin, A. Marshak, W. Wiscombe, J. Martonchik, and R. Myneni published in the *Journal of Atmospheric Sciences*.

Biomass-burning Aerosols in South East-Asia: Smoke Impact Assessment (BASE-ASIA)
Si-Chee Tsay (Si-Chee.Tsay-1@nasa.gov)

Biomass burning has been a regular practice for land clearing and land conversion in many countries, especially those in Africa, South America, and Southeast Asia. However, the unique climatology of Southeast Asia is very different than that of Africa and South America, such that large-scale biomass burning causes smoke to interact extensively with clouds during the peak-burning season of March to April. Every boreal spring the indigenous populations of Laos, Thailand, Vietnam, Myanmar, and southern China clear the ground needed to plant agricultural crops by setting fires. While the fires are often set in areas that are relatively dry with little cloud cover

(particularly in Myanmar, Thailand, and Laos), the smoke plumes they generate can stretch hundreds of kilometers into areas of heavy cloud cover (Vietnam and southern China), as depicted in Figure 5-22. During the springtime, this cloud cover is generally composed of stratiform, low-altitude clouds associated with frontal systems that originate in China. Because both smoke and clouds converge over Vietnam and southern China, darkened (brown colored) clouds are often seen in satellite images during this season as smoke gets transported to areas that contain the low-lying cloud deck.



Figure 5-22. Interaction of smoke aerosols with extended cloud layer, observed by SeaWiFS on 21 March 1999 in Southeast Asia.

It is imperative that we combine measurements from multisensors to obtain optimal information for determining the impact of smoke aerosols on the radiative budget of the Earth-atmosphere system. We have estimated quantitatively the radiative effect, in the presence of clouds, of smoke aerosols from biomass burning activities in Southeast Asia during boreal spring using such technique. We combined the TOA SW and total (SW+LW) flux from CERES with the AI from TOMS and cloud reflectivity from SeaWiFS. We generated a collocated data set by averaging the daily Level-2 data from these three sensors into 0.5° latitude by 0.5° longitude bins (Hsu et al., 2003). Two types of histograms over cloudy regions were then calculated from this data set: one for relatively smoke-free clouds ($AI < 0.1$) and one for smoke-laden clouds ($AI > 1.5$). The results for SW flux and total (SW+LW) flux are depicted in Figures 5-23a and 5-23b, respectively.

Apparently during boreal spring in Southeast Asia, when smoke aerosols are present in cloudy regions, the peak SW flux is observed to shift from $720\text{--}740\text{ W m}^{-2}$ over relatively smoke-free clouds to $620\text{--}640\text{ W m}^{-2}$ over smoke-laden clouds. Such a reduction ($\sim 100\text{ W m}^{-2}$) in outgoing SW flux is substantial in the radiative budget of the atmosphere. This would, in turn, cause a strong warming in the smoke layer above the cloud deck. The corresponding TOA upwelling total flux peaks at about $960\text{--}980\text{ W m}^{-2}$ over smoke-free clouds for this region during March, while the total flux over smoke-laden clouds peaks at $880\text{--}920\text{ W m}^{-2}$. The reduction in the total flux due to the presence of smoke aerosols is around $70\text{--}80\text{ W m}^{-2}$. This is because the LW flux increases by about $20\text{--}30\text{ W m}^{-2}$ over the smoke-laden clouds when compared to that over smoke-free clouds, and thus compensates for some of the reduction in the SW flux, resulting in a slightly smaller net reduction in the total flux. One of the processes that leads to an increase in LW emission, due to the presence of smoke aerosols in cloudy areas, could be an enhancement of the temperature inversion by SW absorption. Such large perturbations in radiation fields (SW + LW) will induce an imbalance in the terrestrial heat budget that could affect local wind

circulation patterns and cloud dynamics. This, in turn, may lead to drastic change when the Southeast Asian monsoon begins, currently in the late boreal spring and early summer. Perturbations in the onset of the Southeast Asian monsoon are believed to have great influence on the development of full-scale Asian summer monsoons during the subsequent months [Lau and Yang, 1997]. Therefore, better quantification of the smoke effect on clouds in the radiative budget is crucial to the improvement of the predictability of the tropical climate system during the boreal spring.

Since this observed radiation perturbation may be a combination of direct effects (absorption of sunlight above the cloud) and indirect effects (mixing and interacting with low clouds), more ground-based and aircraft measurements are urgently needed to fully understand and partition the contributions from both. We are currently initiating a pilot study, BASE-ASIA, in seeking a better understanding of the impact of the biomass burning aerosols on regional-to-global climate, hydrological and carbon cycles, and tropospheric chemistry in Asia.

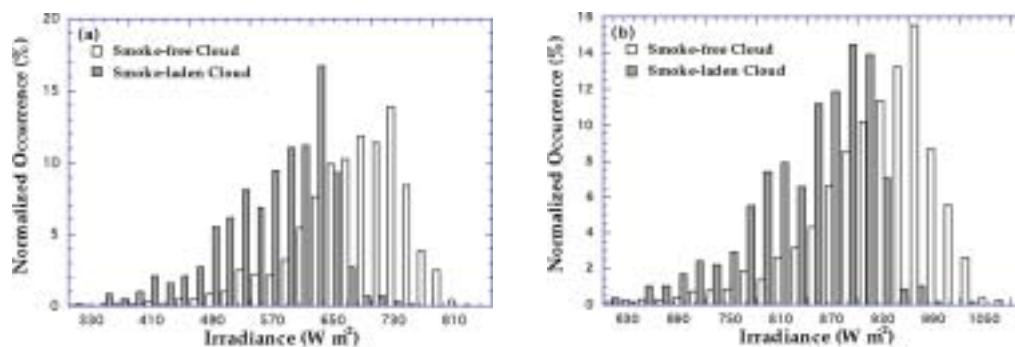


Figure 5-23. Normalized (unity) histograms of the CERES TOA upwelling (a) shortwave, and (b) total (shortwave + longwave) flux for the domain region of (15–30° N, 100–125° E) during the month of March 2000 over smoke-free clouds (nonshaded), and over smoke-laden clouds (shaded). To prevent subpixel (broken) cloud contamination, we adopt a criterion that cloud reflectivity derived from the SeaWiFS 865 nm channel has to be greater than 0.7.

Lau, K.-M., and S. Yang, Climatology and interannual variability of the Southeast Asian summer monsoon, *Adv. In Atmos. Sci.*, **14**, 141-162, 1997.

Hsu, N.C., J.R. Herman, and S.-C. Tsay, Radiative impacts from biomass burning in the presence of clouds during boreal spring in Southeast Asia, *Geophys. Res. Lett.*, **30**, doi:10.1029/2002GL016485, 2003.

Atmospheric Experiment Branch, Code 915

Branch Summary

The Atmospheric Experiment Branch conducts experimental studies to increase our understanding of the chemical environment in our solar system during its formation and to study the physical processes that have continued to shape solar system bodies through time. To achieve this goal, the Branch has a comprehensive program of experimental research, developing instruments to make detailed measurements of the chemical composition of solar system bodies such as comets, planets, and planetary satellites that can be reached by space probes or satellites.

The Branch's accomplishments for 2002 include:

- 1) The Branch continued participation in the CONTOUR mission that was planned to rendezvous with multiple comets and provide a more detailed understanding of the cometary nuclei and the diversity among comets. CONTOUR was a mission in NASA's Discovery line of small mission program for planetary studies. The CONTOUR PI is Professor Joseph Veverka of Cornell University, and the Applied Physics Laboratory (APL) in Laurel, Maryland, managed the development of this spacecraft. The Neutral Gas and Ion Mass Spectrometer (NGIMS) is one of four instruments on this mission. NGIMS was designed and fabricated inhouse at GSFC with collaboration on the analog portion of the flight electronics with the University of Michigan. The instrument was delivered in December 2001 to the Johns Hopkins APL for integration with the CONTOUR spacecraft. CONTOUR was launched in July 2002. Unfortunately, the Solid Rocket Motor failed near the end of its scheduled 50-sec burn causing an explosion that apparently rendered the spacecraft inoperable. Significant activities for the NGIMS instrument team, however, were the completion of the instrument's final processing, assembly, environmental testing and delivery to APL. The NGIMS team also carried out significant participation during spacecraft integration at APL. A replacement mission, CONTOUR II, is being discussed as a possible new mission for the next Discovery proposal opportunity.

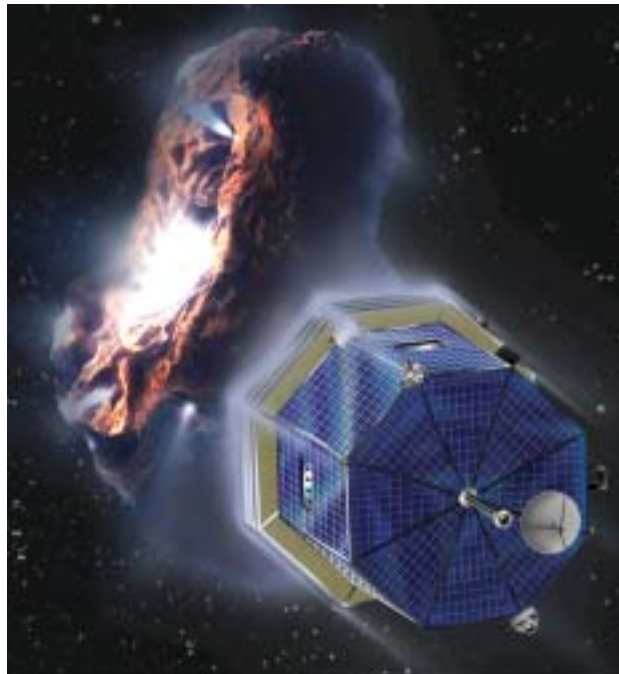


Figure 5-24. Artist's conception of CONTOUR in a rendezvous encounter.

- 2) The Branch continued providing post-launch support for several key planetary missions. These include:
 - A Gas Chromatograph Mass Spectrometer on the Cassini Huygens Probe mission to explore the atmosphere of Saturn's moon Titan.
 - An Ion and Neutral Mass Spectrometer on the Cassini Orbiter to explore the upper atmosphere of both Saturn and Titan.
 - A Neutral Mass Spectrometer on the Japanese Nozomi mission to explore the upper atmosphere of Mars.
- 3) Branch members continued advanced development for measurements on future missions. These include a probe of the deep atmosphere of Venus to carry out precision measurements of isotopes designed to resolve questions of the origin and processing of this atmosphere; a detailed in situ rendezvous mission with the nucleus of a comet to better understand the complexity of organic molecules that might have been delivered to Earth over the course of its history; a landed experiment on Mars to sample isotopes and molecules from its atmosphere and below its surface that can address studies of past climate and the possibility of past life on this planet.
- 4) Branch members are participating in a collaborative astrobiology investigation with the Johns Hopkins Applied Research Laboratory to develop a prototype instrument that will aid in the search for the nature of prebiotic chemistry or evidence of past life. The instrument will be centered around a miniaturized time-of-flight mass spectrometer combined with a gas chromatograph that will allow both simple and complex organic molecules to be resolved. Direct ionization of solid samples using laser ablation or energetic ions combined with electron ionization of gases thermally released from the same samples will allow a wide range of highly volatile to highly refractory components to be analyzed. This powerful technique will enable in situ characterization of organics contained in solid phase material sampled on lander missions to comets, asteroids, Jovian moons, or Mars.
- 5) Branch members developed a mission concept in collaboration with scientists and engineers at GSFC and JPL to carry out measurements for 30 days in the polar region of Mars from a Montgolfiere balloon platform. This mission with the astrobiology focus of a search for pointers to past or present life in the atmosphere, surface, and subsurface was submitted to NASA Headquarters in response to their announcement for this mission.
- 6) Branch members participated in several national and international workshops which focused on a Comet Nucleus Sample Return mission; a Jupiter deep-entry atmospheric probe mission; and an international workshop on Calibration Techniques for in situ Particle Instruments.
- 7) Branch members continued the collaborative effort with GSFC's Engineering Directorate in a comprehensive program to achieve a significant reduction in the size and weight of present-day mass spectrometer systems. This includes reduction to the electronics system by utilizing Application Specific Integrated Circuits (ASICS) and other advanced packaging techniques as well as reductions to the mass spectrometer itself by utilizing MEMS techniques.

Instrument Development: Sample Analysis at Mars (SAM)
Paul R. Mahaffy, (Paul.R.Mahaffy@nasa.gov)

A high priority for the next decade of Mars exploration will be the search for signatures of extinct or extant life (Ardvison et al., 2001, Greeley et al., 2000). A key objective of this exploration will be a search for the location

and characteristics of the range of organic molecules that may reveal the nature of present or ancient biotic or prebiotic processes on Mars. Since the Martian atmospheric and near surface environment is believed to be highly oxidizing where organic molecules may be rapidly destroyed or chemically transformed into more stable organic species (Benner, 2000) this search is expected to focus on samples obtained from protected regions such as the interior of rocks or from below the surface in low permeability sedimentary layers. Chemical fossils might be found, for example, of processes that were in place earlier in the history of Mars when warmer and wetter conditions (McKay and Davis, 1991) might have favored biological activity. Recent advances in understanding the nature of terrestrial microbial life and its ability to adapt to both warm (hydrothermal) and cold (permafrost) environments (Nienow et al., 1993) suggest that the polar ices of Mars may be an excellent target for the search for evidence of extant life. Wherever organic molecules are found, a comprehensive examination of their character will be necessary to address the important question of what role these molecules might have played in Martian biology or prebiotic chemistry. Fundamental studies of organics, reduced species, and isotopes include:

- A general survey of the number and types of discrete volatile organic molecules.
- A characterization of the refractory macromolecular organic material.
- A characterization of the chemical (association with other reducing phosphorus, sulfur, or nitrogen containing species) and mineralogical context of any organic containing samples.
- An identification of the relative abundance of molecular organic species in a homologous series such as alcohols with increasing number of carbon atoms.
- A sensitive test for the presence of molecules of special relevance to biology such as amino acids.
- A test for the predicted stable intermediate oxidation products (such as carboxylic acids) that might be produced from reactive molecules such as amino acids.
- A determination of the chirality of the molecular species identified.
- A characterization of the isotopic composition of the light elements H, C, O, S, P, and N in organic molecules and other reduced species.
- A characterization of the light isotope composition in minerals and a comparison with the same elements in the atmosphere, that might address studies of atmospheric loss to surface reservoirs and to space and atmosphere exchange with the surface.
- A characterization of the light isotope composition in minerals that might distinguish an abiotic production mechanism from evidence of biomineralization.

With several sources of NASA and CNES support we are developing several of these techniques to address astrobiology/organic studies in a Mars surface lander experiment such as the planned 2009 Mars Science Laboratory (MSL). The instrument suite, Sample Analysis at Mars (SAM), will be designed to carry out a detailed in situ chemical and isotopic analysis of solid phase material sampled from the surface or subsurface of Mars. A special focus of SAM is on the detection and analysis of trace organic species that may reveal the nature of ancient biotic or prebiotic processes on Mars together with a sensitive and detailed study of atmospheric gas. With SAM we initiate a program to extend previous NASA and CNES collaborations in the area of geochemical and exobiological investigations to future exploration of Mars. We specifically target this development for the 2009 Mars Science Laboratory Mission. Members of our international team include several scientists and instrument specialists who developed similar capability for the Cassini/Huygens mission. The SAM development team will bring together a unique set of scientific and analytic capabilities to address outstanding questions in Mars exploration. Development support for this program has been provided from both the NASA and CNES. The SAM development is an international collaboration with several participating institutions. The technical development will be led by scientists at GSFC, the University of Paris (with support from CNES), the Service d'Aéronomie (SA), and the Johns Hopkins University Applied Physics Laboratory (JHU/APL).

Atmospheric Chemistry and Dynamics Branch, Code 916

Branch Summary

The Atmospheric Chemistry and Dynamics Branch conducts research in the distribution and variability of atmospheric ozone: 1) by making new measurements; 2) by analyzing existing data; and 3) by theoretically modeling the chemistry and transport of trace gases that control the behavior of ozone. An emerging research focus is on the characterization of sources, sinks, and transport of aerosols, carbon dioxide, and ozone in the troposphere. The Branch's accomplishments for 2002 include the following:

- 1) Branch scientists continued to play key roles in the WMO/UNEP assessment of the stratospheric ozone depletion. This congressionally mandated assessment, held every 3 to 4 years, brings together experts in stratospheric research to assess the current health of the ozone layer and to make informed predictions about its future state. A key input to this assessment is the long-term global record of ozone created by combining ground-based and satellite data developed by the Branch. An emerging focus is to use the 3-D chemistry and transport model developed in the Branch to study the impact of greenhouse warming on the stratosphere.
- 2) The Branch manages the TOMS project, which along with the SBUV project (a collaborative effort between NASA and NOAA, and supported by the Branch) continues the highly acclaimed ozone time-series. In 2002, advanced algorithms (version 8) to process SBUV and TOMS data were developed under the leadership of Branch scientists. These algorithms are expected to significantly improve the utility of these datasets for atmospheric chemistry research. In addition, Branch scientists continued to improve the quality of several popular datasets produced from TOMS to study global air quality, viz., aerosols, surface UV, and tropospheric ozone.
- 3) Branch scientists led the development of the 2nd SAGE III Ozone Loss and Validation Experiment campaign (SOLVE II), an aircraft field campaign in the northern polar region designed to improve our understanding of the transport and chemistry of the arctic region and to provide data for the validation of the recently launched SAGE III instrument. Branch scientists provided the stratospheric ozone, temperature, and aerosol Lidar for this campaign.
- 4) Several Branch scientists are members of the International OMI science team. OMI is a Netherlands-provided instrument, scheduled to fly on the EOS Aura satellite in early 2004. This team participated in developing a 4-volume description of the scientific algorithms that will be used to process OMI data to derive a variety of products relevant in atmospheric chemistry research. This document received good reviews from a panel of experts selected by the EOS Project Office.
- 5) The Branch manages the SHADOZ (Southern Hemisphere Additional OZonesondes) program. This international program has greatly improved the quality and quantity of ozone vertical profile data in the region of the world that is experiencing rapid environmental change. The Branch scientist who leads this effort, Anne Thompson, was recently awarded a Fellowship of the American Association for the Advancement of Science (AAAS), based partly on her work related to SHADOZ.
- 6) Branch scientists have developed a state-of-the-art model, called GOCART, to study global distribution and transport of aerosols. This model is proving invaluable in interpreting aerosol data derived from TOMS, SeaWiFS, and MODIS.

The following two articles illustrate some of the science resulting from field campaigns the Branch is heavily involved in.

Zonal Wave-one Structure in Tropical Ozone Observed in SHADOZ (Southern Hemisphere Additional Ozonesondes) Network Data

Anne Thompson (Anne.M.Thompson@nasa.gov)

Although the launch of the first total back-scattered ultraviolet (BUV) satellite more than thirty years ago initiated space-era ozone measurements, validation of column and profile ozone is a more recent development, which requires deployment of ground- and balloon-borne instrumentation. Approximately 100 stations worldwide regularly launch an electrochemical concentration cell (ECC) ozonesonde, in which air pumped through cells with potassium iodide solutions produces a current proportional to the amount of ozone; the ozonesonde is flown with a standard radiosonde. Most ozonesonde stations are in northern mid-latitudes. The only tropical station that has operated since the 1970's is at Natal, Brazil, where launches are supported by a partnership between the Goddard/Wallops Upper Air Group and INPE (the Brazilian Space Agency).

To end the lack of tropical ozone profile data, the SHADOZ (Southern Hemisphere ADditional OZonesondes) project was initiated in 1998 by personnel in GSFC's Laboratory for Atmospheres and Laboratory for Hydro-spheric Processes, NOAA's Climate Diagnostics and Monitoring Laboratory, and more than a dozen sponsoring nations. Through augmentation of ozonesonde supplies, SHADOZ facilitates weekly launches at a dozen locations (see map in Figure 5-25), collecting and disseminating all data through a centralized archive at the Web site: code916.gsfc.nasa.gov/data_services/shadoz. More than 1600 ozone and PTU (pressure-temperature-humidity) profiles are available at the SHADOZ archive. In addition to enhancing the satellite ozone profile climatology, SHADOZ data are used to study tropical chemistry and dynamics. This has led to a breakthrough in a decade-long scientific argument about the location and origins of a zonal "wave-one" pattern in total ozone that was first detected in TOMS satellite data. The "wave-one" refers to a greater total ozone column amount over the Atlantic and adjacent continents than over the Pacific. Is the "wave-one" due to relatively more Atlantic ozone in the stratosphere or in the troposphere? This question is answered through the vertical resolution of the sonde data and longitudinal coverage of SHADOZ. The zonal structure (Figure 5-26) shows that the "wave-one" results from an ozone excess in the troposphere. Free tropospheric ozone has a lifetime up to a month or more and the general pattern in Figure 5-26 persists throughout the year. Continuing studies with models and correlative data are focusing on the mechanisms causing the wave. Some of the higher ozone features in the lower mid-troposphere are due to photochemical ozone from biomass fires. Convection takes low-ozone (unpolluted) air from boundary layer to upper troposphere over Watukosek (Java), with components of tropical general circulation also contributing to the mean ozone distribution.

Thompson, A.M., et al., The 1998–2000 SHADOZ (Southern Hemisphere ADditional OZonesondes) tropical ozone climatology. 2. Tropospheric variability and the zonal wave-one, *J. Geophys. Res.*, 10.129/2002JD002241, in press, 2002.

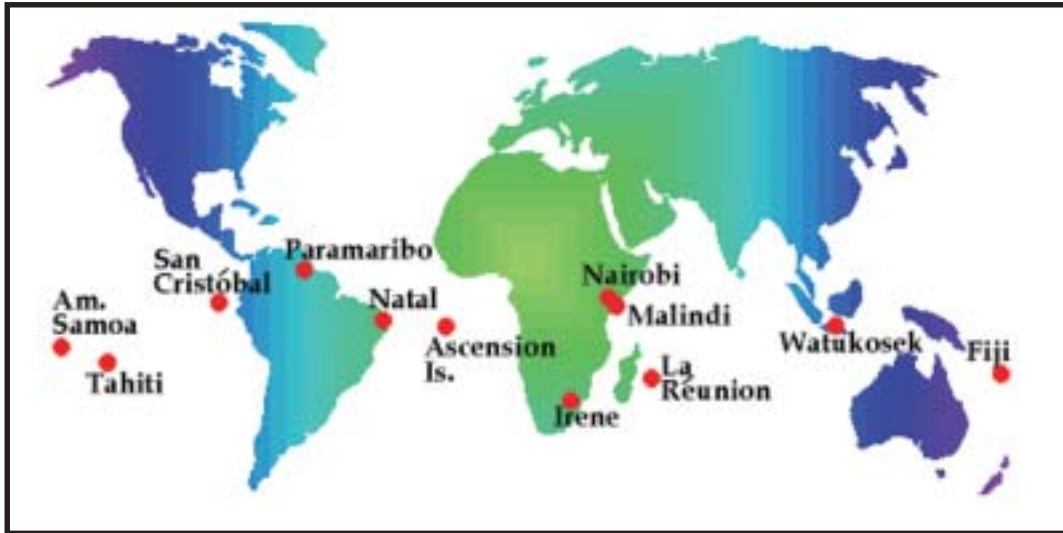


Figure 5-25. SHADOZ sites. The results in Figure 5-23 are based on more than 1100 soundings taken in 1998–2000 at all the stations except Paramaribo and Malindi.

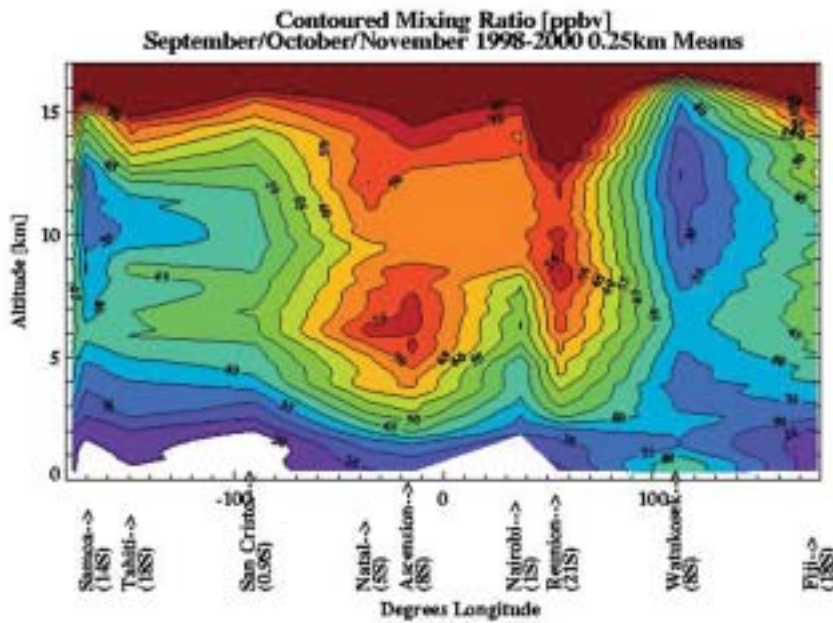


Figure 5-26. The tropospheric “wave-one” pattern in tropospheric ozone results from the structure shown for September–October–November (SON) with mixing ratio contours based on 0.25-km averaged segments.

GSFC Participation in the Second SAGE-III Ozone Loss and Validation Experiment (SOLVE-II).
Paul A. Newman (Paul.A.Newman@nasa.gov)

The SAGE III Ozone Loss and Validation Experiment (SOLVE II) was a measurement campaign designed to examine the processes controlling ozone levels at mid- to high latitudes. The mission also acquired correlative data needed for the validation of the Stratospheric Aerosol and Gas Experiment (SAGE) III satellite measurements. SAGE-III is a NASA instrument on board a Russian Meteor-3 satellite platform. SAGE-III is primarily used to quantitatively assess high-latitude ozone loss.

The SOLVE II mission was primarily conducted during January 2003. Measurements were made in the Arctic high-latitude region during winter using the NASA DC-8 aircraft, as well as balloon platforms and ground-based instruments. The NASA DC-8 was based in Kiruna, Sweden, slightly north of the Arctic Circle.

GSFC scientists participated in SOLVE II in 3 ways: the Airborne Raman Ozone, Temperature and Aerosol Lidar (AROTAL) instrument, project support, and flight planning. Thomas McGee and John Burris were co-principal investigators on the AROTAL instrument, Paul Newman and Mark Schoeberl served as project scientists for the NASA DC-8, and Leslie Lait performed flight planning for the DC-8.

Integration of instruments onto the DC-8 began in mid-November 2002 and was completed in early December. Four test flights of the entire payload were flown from NASA Dryden Flight Research Center in California, and the DC-8 arrived in Kiruna, Sweden, on January 9, 2003. A total of 11 science flights were conducted in Kiruna, and the DC-8 returned to NASA Dryden on February 6, 2003.

Ozone loss in the polar stratosphere is directly caused by catalytic chlorine and bromine reactions. The high levels of reactive chlorine occur because of reactions of reservoir chlorine species on the surfaces of polar stratospheric clouds (PSCs). PSCs were observed by the NASA DC-8 lidar systems on the flight of January 9, 12, 14, and February 4, 2003, at altitudes between 65,000 and 80,000 feet. In Figure 5-27, we see a PSC cloud that was observed over southern Sweden on January 14, 2003. Three types of PSCs are common in the polar region: type Ia (small crystals), type Ib (small liquid droplets), and type II (large crystals). The type Ia PSCs are probably nitric acid hydrates, the type Ib are probably solutions of nitric acid, water, and sulfuric acid, while the type II PSCs are water ice crystals. The PSC in Figure 5-27 is probably a water ice cloud because of the strong coloration from the ice crystal refraction.



Figure 5-27. Picture of PSC taken from the NASA DC-8 over southern Sweden on January 14, 2003. Photo by Paul A. Newman.

Two chlorine compounds (HCl and ClONO_2) that normally do not destroy ozone can collect on the surfaces of PSC particles. On these surfaces, chemical reactions convert the HCl and ClONO_2 to Cl_2 and HNO_3 . With a small amount of sunlight, the Cl_2 is broken down and begins to catalytically destroy ozone. During the winter of 2002–2003, the polar vortex was cold and had moved southward toward Europe, exposing the air to sunlight. Normally, ozone values in the core of the vortex near 20 km would be approximately 3 parts per million. However, because of the high levels of reactive chlorine, ozone steadily decreased over the course of the month. Figure 5-28 displays ozone values observed on the flight from Kiruna, Sweden, to California on February 6, 2003. The x-axis of the figure shows the time, while the y-axis shows altitude. The polar vortex was situated over Kiruna, such that ozone values at 20 km on the left of the figure are inside the polar vortex. Typically values of ozone inside the vortex in January would be near values of 3000 ppbv (the aqua color). However, during early February, these values are near 1500 ppbv, suggesting very large ozone losses inside the polar vortex.

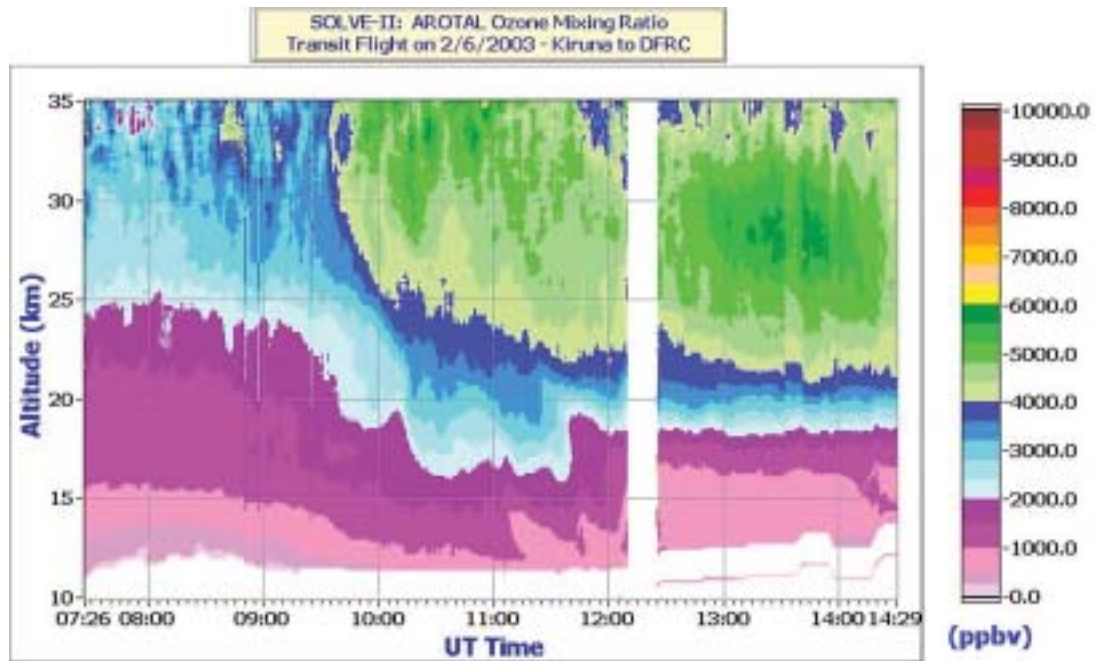


Figure 5-28. Ozone values observed on the flight from Kiruna, Sweden, to California on February 6, 2003, from the GSFC AROTAL instrument.

These initial results are qualitative, and will require further processing and quantitative analysis. These SOLVE II results will be directly used to quantify ozone loss in the vortex. The ozone values and ozone loss will then be compared to the SAGE III ozone values to validate our global observations of ozone.